Heliophysics Senior Review 2008

The Reuven Ramaty
High Energy Solar Spectroscopic Imager
(RHESSI)

Robert Lin, Principal Investigator

Brian Dennis, Mission Scientist

Manfred Bester, Mission Operations Manager

Bryan Mendez, E/PO Manager

Table of Contents

1 EXECUTIVE SUMMARY

The RHESSI Small Explorer mission is designed to investigate particle acceleration and energy release in solar flares through imaging and spectroscopy of hard X-ray (HXR)/gamma-ray continua emitted by energetic electrons, and of gamma-ray lines produced by energetic ions. The single RHESSI instrument provides ground-breaking imaging and spectroscopy measurements over the broad energy range from soft X-rays (3 keV) to gamma-rays (17 MeV).

RHESSI was launched in February 2002, and has been operating successfully ever since. Over 11,000 flares with detectable emission have been identified above 12 keV, ~950 above 25 keV, and 30 above 300 keV with 18 showing gamma-ray line emission. In addition over 25,000 microflares have been detected above 6 keV. Since the start of the mission, all the data and the analysis software have been made immediately available to the scientific community.

RHESSI provides unique observations of high-energy processes close to the Sun that address the key goals of the Heliophysics Great Observatory: understanding the fundamental processes of particle acceleration and energy release in solar eruptions, both flares and CMEs. The resulting photon emissions and accelerated particles directly affect our Home in Space, and are especially important for our Journey Outward.

In the ~2 years since the last Senior Review, analysis of RHESSI observations has resulted in over 200 publications, and many press releases, popular articles, and awards. Some of the new results include:

- The first comprehensive survey of ~25,000 hard X-ray microflares, providing their occurrence frequency vs. energy, both thermal and non-thermal, and showing that essentially all of them occur in active regions, and that they generally show steep non-thermal spectra.
- The best upper limits on the hard X-ray emission of the quiet Sun, >2 orders of magnitude lower than the weakest microflare. These upper limits constrain the production of axions (a dark matter candidate) in the Sun's core, thus limiting the axion-photon coupling constant.
- The discovery of non-thermal hard X-ray sources very high (up to >0.3 Rs) in the corona (when the associated flare is occulted) accompanying all fast (>~1000 km/s) coronal mass ejections (CMEs).
- The first survey of partially disk-occulted flares, showing rapid variations of the coronal non-thermal HXR emission (likely thin-target emission without significant collisional energy losses), often well above the thermal source.
- The detection of X-ray source motions, first from the flare looptop down the legs and then back up, likely related to chromospheric evaporation.
- The discovery of large numbers of relativistic electrons with extremely hard spectra in coronal loops above the footpoints in large flares.
- The first measurements (with ~2σ significance) of polarization of ~100-350 keV X-rays in large solar flares.
- The finding of a very close linear correlation between >0.3 MeV gamma-ray continuum and 2.223 MeV neutron-capture line fluences, indicating that the acceleration of the parent relativistic electrons and >~30 MeV protons must be closely related.
- The development of powerful new model-independent mathematical methods to infer the energy spectra of the parent electrons as well as information on their angular distribution, from the uniquely precise RHESSI X-ray measurements.
- The development of plasma theory and simulations of the magnetic reconnection process in flares that directly accelerate electrons with high efficiency, as required by RHESSI and previous observations.
- The discovery of a close correlation between the >50 keV power law spectral indices of energetic electrons in prompt impulsive events observed by the Wind 3DP at ~1 AU and of the associated flare HXR burst, indicating a common source.
- The discovery that the excess solar oblateness detected by RHESSI's SAS (solar aspect sensor) may be due to low level faculae that cover the entire solar disk and not just the active latitudes.
- The discovery that the electrons up to 30 MeV that produce Terrestrial Gamma-Ray Flashes (TGFs) are accelerated at 13-15 km altitude, and that some of the electrons enter the magnetosphere.

The numerous results over the RHESSI lifetime have changed our perspective on solar flares, particularly on high-energy processes in flares. The most recent RHESSI workshop in June 2007 was devoted to planning for a ~500-page book, to be published by Space Sciences Reviews (for easy access). Most of the chapter drafts are finished, and publication is expected later this year.

The spacecraft and instrument continue to operate nominally. After five and a half years RHESSI's germanium detectors were showing strong effects of radiation damage, as predicted, including significant loss of active volume. The detectors were annealed in November 2007 by heating up to >~90º C for a week, and they have recovered close to their full sensitive volume and to the high energy resolution they had in

2005. Further anneals are planned as needed to maintain acceptable detector performance. Since the mission was designed with no expendables and the orbit decay has been minimal, RHESSI should be able to operate for years to come. Thus, RHESSI is ready for the rise from solar minimum to the expected maximum of the next activity cycle in 2009-2012.

The recent successful launches of Hinode and STEREO bring unique new observations that are highly complementary to RHESSI for the study of solar flares, CMEs, and solar energetic particles. In particular, Hinode provides the previously missing high cadence measurements in broad–band soft X-rays, diagnostic EUV spectroscopy, and optical/ vector magnetograph required for flare studies; while STEREO provides stereo EUV imaging of flares, coronagraph imaging of CMEs, radio burst tracking, and multi-point in situ measurements of energetic particles and plasma/fields. The launch of the Solar Dynamics Observatory later this year will add the full-Sun, high cadence, multi-wavelength imaging of the Sun. Finally, the launch of GLAST later this year will provide complementary measurements of ultra-high-energy gamma-rays from solar flares. Thus, for the first time the elements of the Heliophysics Great Observatory (HGO) required for comprehensive studies of energy release and particle acceleration processes in flares and CMEs will be available.

We propose a Solar High Energy Events GI program to maximize the science return by supporting studies (not possible under the in-guide funding) that integrate the remarkably complete suite of new high-energy and supporting observations of solar explosions, and their energetic consequences obtained by the HGO in this upcoming rise to solar maximum.

2 SCIENCE

The past two years have been tremendously productive scientifically for the RHESSI mission. RHESSI has provided (and continues to provide) an enormously rich data set. A detailed description of the RHESSI mission, instrument, and software is given in the first six papers of the Nov. 2002 issue of Solar Physics (vol. 210, p. 3-124). Here is a brief summary.

RHESSI provides high-resolution imaging and spectroscopy of bremsstrahlung X-ray/gamma-ray continuum emitted by energetic electrons, and gamma-ray lines produced by energetic ions. At HXR and gamma-ray energies, the only viable method of obtaining arcsec-class images within the SMEX constraints is with Fourier-transform imaging. The RHESSI instrument has an imager made up of nine Rotating Modulation Collimators (RMCs), each consisting of a pair of widely separated grids mounted on a rotating spacecraft, to achieve angular resolution as fine as ~2 arcsec and imaging up to gamma-ray energies. Behind each RMC is a segmented germanium detector (GeD) to detect photons from 3 keV to 17 MeV. The GeDs are cooled to ~90 K by a space-qualified long-life mechanical cryocooler, to achieve the high spectral resolution (~1 to 10 keV FWHM). The GeDs were successfully annealed in November, 2007, to mitigate radiation damage.

As the spacecraft rotates, the RMCs convert the spatial information from the source into temporal modulation of the photon counting rates of the GeDs. Pointing information is provided by the Solar Aspect System (SAS) and redundant Roll Angle Systems (RASs). An automated shutter system allows a wide dynamic range ($>10^7$) of flare intensities, from microflares to the largest X-class flares, to be handled without instrument saturation, and it allows the sensitivity to be maximized when low-energy (<~20 keV) X-ray fluxes are low. The spin-stabilized (~15 rpm) spacecraft is Sun-pointing to within ~0.2º and operates autonomously, with the energy and time of arrival for every photon stored in a solid-state memory (sized to handle the largest flare) and telemetered to the ground.

The RHESSI observations provide powerful diagnostics because: 1) they combine high spatial resolution, high spectral resolution, and excellent precision; 2) they span an enormous energy range from soft X-rays (~3 keV) emitted by hot thermal plasmas, through the hard X-ray/gamma-ray continuum emitted by accelerated electrons, to gamma-ray lines emitted by accelerated ions; 3) data for every detected count are brought to the ground so there is unlimited flexibility in the data analysis; and 4) the X-ray and gamma-ray emission processes are quantitatively well-understood.

Thus, significant effort over the past two years was devoted to inferring the parent electron distribution in energy, angle, time, and space from the RHESSI X-ray measurements. The methods developed take into account the effect of albedo – scattering of the photons from the dense photosphere – on the X-ray spectrum. This also allows information on the directivity of the electrons to be inferred, and to correct for it in deriving the parent electron source spectrum. Recently, a new technique has been developed that utilizes the imaging spectroscopy measurements to go directly to the parent electron distribution in energy and space.

The observations appear to be generally consistent with the flare electron (and ion) acceleration being intimately related to the magnetic reconnection. For many flares the accelerated tens of keV electrons contains >~10-50% of the total energy released in the flare. Since reconnection ideally results in bulk flows, a long-standing question is how can the energy released

be converted to energetic electrons. In the last couple of years this problem has been addressed by leading plasma theorists and simulation experts, and a possible explanation has been put forward that arises naturally from the reconnection process, and that also appears to explain electron acceleration in a reconnection event observed in situ in the Earth's deep magnetotail.

Another puzzle has been the detection of HXR emission only at a few footpoints while optical/EUV emissions are seen along the entire ribbons of the flare loop arcade. Recent detailed analyses of RHESSI observations with the finest spatial resolution show HXR emission along the entire loop arcade. It's not yet clear whether the normal lack of ribbon HXR emission is due to dynamic range limitations of RHESSI's imaging.

In the past two years there have been systematically searches for relatively weak coronal HXR emission when the flare is occulted by the limb. Coronal non-thermal emissions are found to be common – above flare loops and behind fast CMEs. Furthermore, at high energy (>~200keV) HXR emissions seem to be stronger in the corona compared with tens of keV emissions.

Comparisons of RHESSI HXR observations with Wind energetic electron observations for prompt impulsive SEP events show that the >50 keV HXR spectra are closely correlated to the escaping electron spectra, suggesting a common source for the HXR-producing and escaping electrons. However, the relationship is not consistent with standard thick or thin target models.

Finally, the approach to solar minimum in the last few years has been ideal for systematic studies of microflares and their implications for coronal heating, and of quiet Sun (no active regions) X-ray emissions. With the attenuators out RHESSI provides uniquely high sensitivity at 3-20 keV energies.

In addition, RHESSI's Solar Aspect System (SAS) has provided the best solar optical shape measurements ever obtained, opening up a new area of research. RHESSI's discovery that TGFs commonly extend up to >~20 MeV has revitalized the study of lightning related high-energy phenomena. Finally RHESSI provides unique measurements for a variety of astrophysical high-energy phenomena.

To tap the real power of RHESSI requires the integration of its data with that of the other HGO missions and with the Gamma-ray Large Area Space Telescope (GLAST) that will be launched in a few months. To understand what is special about the flare and CME-related particle acceleration and energy release regions identified by RHESSI, we need good magnetic field models based on accurate vector photospheric (and chromospheric if available) measurements. We need information on the magnetic topology, waves, shocks, and ambient conditions in the corona obtained by instruments on Hinode and STEREO, as well as on TRACE, SOHO, and groundbased observatories; SDO will soon provide additional capabilities. To understand the Sun's connection to the heliosphere will require ACE, Wind, STEREO, SOHO, Ulysses and other spacecraft measuring energetic particles, radio emission, magnetic fields, and the solar wind. We want to understand what conditions lead to these high-energy eruptive phenomena. To further the joint analysis of the many events expected to be observed in common, the RHESSI team is proposing a GI Program specifically for this purpose. A joint workshop is already planned for December 2008 in Napa, CA, to discuss the results of the early cross-platform (RHESSI, Hinode, STEREO) observations. Preliminary results (see below) already show the promise of such multi-platform comparisons.

2.1 Accomplishments

To date, there have been over 670 papers and at least 25 PhD theses published using RHESSI data. They cover a very wide range of topics so we are only able to highlight some of the areas of current research.

2.1.1 Hard X-rays & Parent Electrons

2.1.1.1 Photospheric Compton Scattering of X-rays (Albedo)

The observed hard X-ray emission from solar flares is a combination of primary bremsstrahlung photons with a reflected component from dense layers of solar atmosphere of the downward-directed primary emission. This backscattered component can be significant, creating new features and/or distorting or masking features in the primary spectrum, and so substantially modifying key diagnostics such as the electron spectrum or electron energy budget. This effect is well-known in solar physics, and more generally in X-ray astronomy, and it has been widely studied theoretically (e.g., Tomblin, 1972; Santangelo et al., 1973; Bai and Ramaty, 1978). But it is only with the remarkably precise RHESSI measurements that photospheric albedo can be detected and studied in the X-ray spectrum (Kasparova et al 2005, Kontar et al, 2006) and in X-ray images (Schmahl and Hurford, 2003). It is straightforward to calculate the albedo by Monte-Carlo simulations (e.g. Bai and Ramaty, 1978) if the primary X-ray spectrum is known. However, the primary spectrum is unknown and unlikely to be an exact power-law, as is sometimes assumed. Kontar et al. (2006) have developed a Green's function approach to the backscatter spectral deconvolution problem -

constructing a Green's matrix including photoelectric absorption - that allows a spectrum-independent extraction of the primary spectrum from the spectrum observed by RHESSI. The method is now a fully integrated part of the RHESSI OSPEX software package.

As a result of the dependence of the albedo component on the heliocentric angle (the albedo contribution should be stronger for disk events as compared to limb events), the shape of photon spectra should vary as a function of their position on the solar disk (Bai and Ramaty, 1978; Kontar et al., 2006). A statistical analysis of RHESSI flares (Kasparova et al., 2007) demonstrates a clear center-to-limb variation of photon spectral indices in the 15 - 20 keV energy range and a weaker dependency in the 20 - 50 keV range. The observed spectral variations were found to be consistent with the predictions of albedo-induced spectral index changes.

The albedo spectral "contaminant" in fact can provide information on the anisotropy of the flare fast electron distribution, by providing a view of the hard X-ray flare from behind, like a dentist's mirror. Moreover, the solar albedo "mirror" is spectrally distorting, resulting in an albedo "bump" feature, the strength of which is an indicator of the degree of downward beaming of the electron distribution. This solar "mirror" allows us to obtain information on the directionality of the primary X-ray source, and therefore on the accelerated electron distribution, from a single spacecraft. Application of this spectrometry method to two strong flare X-ray bursts (Kontar and Brown, 2006) observed by RHESSI shows that the ratio of downward and upward propagating X-ray emitting electrons is close to one in a wide range of energies.

In the standard thick-target flare model, electrons are accelerated high in the corona and travel down the loop field lines to the dense chromosphere where they produce the observed flare hard X-ray emission. The isotropization (and energy loss) of the downward electron beam is due to the collisions only and hence isotropy is only approached when electrons have lost most of their energy and are therefore no longer emitting very energetic radiation. The lack of a strong electron beaming, inferred from RHESSI data for these two intense flare hard X-ray bursts close to disk centre events (Kontar and Brown, 2006), rules out the basic thick-target model that has been around for decades, unless the electrons are effectively isotropized somehow. For example, X-ray source electrons could be locally and continuously reaccelerated with near isotropy along the entire length of a magnetic loop. Such a model would also solve other difficulties of the thick-target model, such as the problematic high beam density and currents involved.

More recently, in a study of nine flares showing spectral flattening at low energies, Sui et al. (2007) found that albedo from isotropically emitted photons could account for this flattening in only three of the flares, all located near disk center where the contribution from albedo is greatest. We note here that for some flares, RHESSI can directly measure the albedo component to provide information on the height of the HXR source and its directivity.

Kontar et al. (2007) have shown that the quality of the RHESSI spectra at energies >300 keV is sufficient to clearly identify the role of electron-electron bremsstrahlung in the hard X-ray spectrum, and to modify the parent electron flux distribution accordingly. Application of their method shows that previously unexplained "breaks" in flare electron spectra may simply be an artifact of neglecting this important component of the emission.

Kontar, E.P., Emslie, A.G., Massone, A.M., Piana, M., Brown, J.C., & Prato, M. 2007, Ap.J., 670, 857.

Sui, L., Holman, G. D., and Dennis, B. R. 2007, ApJ, 670, 862.

2.1.1.2 New Imaging Spectroscopy Methods

One of the main science goals of RHESSI is ***imaging spectroscopy***, the production of an "image cube" of HXR intensity I versus 2-D position (x, y) and photon energy ε. Knowledge of the cross-section for the hard X-ray emission process then allows us to transform this into the real science goal – a map of the accelerated electron flux spectrum F versus (x, y) and electron energy E. Over the past year or so, major advances in this transformation have been made.

RHESSI stores imaging information through the temporal modulation of flux by the nine sets of rotating grid pairs. This information is most readily translated into visibilities, two-dimensional spatial Fourier transforms of the image (Hurford et al. 2002, 2008). "Traditional" imaging spectroscopy then proceeds by "stacking" count-based images at different ε and examining the hard X-ray intensity $I(\varepsilon)$ in prominent features. However, this method has several drawbacks. First, it does not fully optimize the way in which spatial information is encoded by RHESSI. This is because the inferred flux in any feature (or spatial region) is determined by a mix of a finite number of spatial Fourier components which also extend beyond the feature under scrutiny. Thus, there is not only a loss of information due to limited spatial frequency sampling but also contamination due to Fourier sidelobes from neighboring features. Second, since the counts in different energy ranges are independent statistical quantities, there is no a priori guarantee that,

in the presence of statistical noise, images will vary smoothly with photon (or count) energy, as they must in the physical case of an electron flux that does vary smoothly with energy.

A new imaging spectroscopy technique (Piana et al. 2007) has recently been developed which overcomes these difficulties and produces the desired "information cube" F(x, y; E). The method accomplishes the transformation from count data to electron flux information by performing a regularized spectral inversion on the count spectrum at sampled points in the spatial frequency domain, i.e., on the photon (or count) visibility spectra V(u, v; ε). This algorithm demands smoothness in the electron spectrum at each spatial frequency point, thus enhancing patterns that persist over a relatively wide energy band, while suppressing noise-related signals that are present only over a narrow range of energies. Well-established image reconstruction techniques (Hurford et al. 2002) can then be applied to the resulting "electron flux visibilities" W(u, v; E) to produce the desired "electron flux images" F(x, y; E). Since the visibilities used to construct these electron flux images are obtained using a regularized inversion technique, they, and their corresponding "electron images," will, by construction, vary smoothly with E. We can then reliably infer physically plausible electron spectra in prominent spatial features by "stacking" the recovered electron images.

2.1.1.3 HXR Emission Along Flare Ribbons

One of the best examples of the use of RHESSI's imaging spectroscopy with the finest grids is shown in fig. 2.1.1-1 for the M8.0 flare on May 13, 2005 (Liu et al. 2007a, b, 2008; Jing et al. 2007). This event was sufficiently intense and showed significant modulation in the count rates of all nine detectors to allow fine structure at the 2-arcsecond level to be imaged. Remarkably, the 25 – 50 keV image shows the emission extending along the full extent of the ribbons and closely matches the TRACE 1600 Å brightenings. This is in contrast to the more usual situation earlier in this flare and in many other flares where just one or two bright HXR footpoints are seen on each EUV or Hα ribbon. Presumably, in those cases, energetic electrons are precipitating at all points along the ribbons but only the brightest points show up in the RHESSI images because of its limited dynamic range of <50:1. At the time of the image shown in fig. 2.1.1-1, the flux of precipitating electrons was sufficiently uniform along the ribbons to allow their presence to be revealed at all locations in the HXR image. The 6 – 12 keV contours show the usual high–temperature (~20 MK) source extending along the top of the arcade of loops that produce the ribbons.

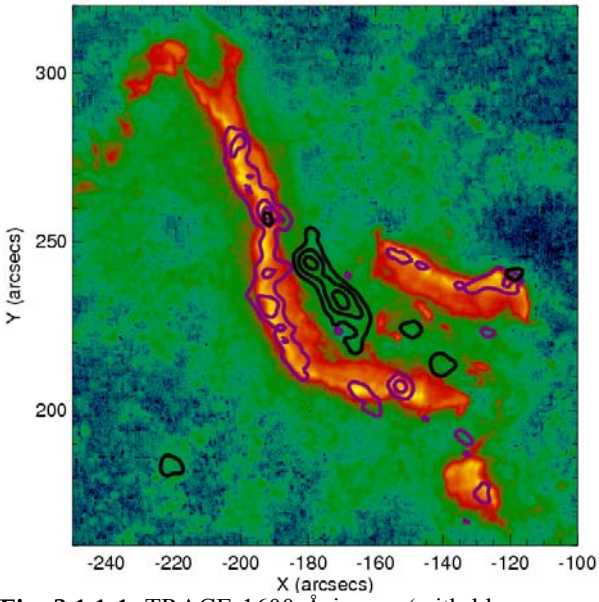

Fig. 2.1.1-1. TRACE 1600 Å image (with blue-green-red-yellow color scale) near the peak of the two-ribbon GOES M8 flare at 16:45:28 UT on 13 May 2005. The overlaid contours show the 6 – 12 keV (black) and 25 – 50 keV (purple) sources obtained from one-minute integrations of RHESSI data about this time. The RHESSI images were reconstructed using the CLEAN algorithm with modulated count rates equally weighted for all nine subcollimators, giving a resolution as fine as the 2 arcsecond (FWHM) capability of the finest grids. The TRACE image has been moved by 2 arcsec in X and 5 arcsec in Y to provide the best match to the RHESSI 25 – 50 keV sources.

This 13 May 2005 event was associated with an EUV sigmoid eruption, and the extensive observations have been analyzed in detail by Liu et al. (2007a, b, 2008) and Jing et al. (2007). They have attempted to explain why the HXR sources appear first as one or two individual bright footpoints but later extend relatively uniformly along the full extent of the ribbons. Early in the event when only one or two point-like HXR sources were seen on each ribbon, Jing et al. (2007) found a good spatial correlation between the HXR flux and an energy release rate consistent with the standard 2D reconnection model. They suggest that tether-cutting reconnection first occurs between the two elbows in the middle of the sigmoid, resulting in electron acceleration concentrated on a few field lines and the HXR sources appearing footpoint-like, as usual (e.g. Moore et al. 2001). Later on, reconnection takes place in the current sheet above the magnetic arcade of loops and the accelerated electrons bombard the chromosphere all along the footpoints of the arcade, resulting in the ribbon-like HXR emissions. Exploiting RHESSI's capability of imaging spectroscopy in each pixel, Liu et al. (2008) further found a spatial

anticorrelation relationship between the local HXR flux and the local spectral index. They suggested this as a spatial analog of the temporal soft-hard-soft spectral evolution pattern of the integrated HXR flux, which may contribute to explaining the usual confined nature of HXR sources compared with extended Hα/UV ribbons. They also found an anticorrelation between the HXR spectral index and the inferred convestive electric field along the ribbon.

Emslie, A. G. et al. 2003, ApJ., 595, L107.
Hurford, G. J., et al. 2002, Sol. Phys., 201, 61
Hurford, G. J. et al. 2008, in preparation.
Jing, J. et al. 2007, ApJ, 664, L127
Liu, C. et al. 2007a, ApJ, 658, L127
Liu, C. et al. 2007b, ApJ, 669, 1372
Liu, C. et al. 2008, ApJ, 672, L69.
Moore et al., ApJ 552, 833, 2001
Piana, M., et al. 2007, ApJ, 665, 846.
Sui, L, et al. 2002, Sol. Phys., 210, 245

2.1.1.4 Electron Acceleration During Magnetic Reconnection

HXR observations show that the accelerated tens-of-keV electrons often contain >~10-50% of the total energy released in the flare, implying that electron acceleration is intimately related to the energy release process (Lin & Hudson, 1971), presumably magnetic reconnection. Electron acceleration to hundreds of keV is also observed inside the reconnection region in the Earth's deep magnetotail (Oieroset et al, 2002). In the last few years, very significant progress has been made in the understanding of collisionless magnetic reconnection, through in situ space measurements, laboratory studies, and extensive theory and simulation work. Recently, the long-standing problem - to explain how energetic electrons are efficiently produced as magnetic fields reconnect and release energy - has been addressed by Drake et al (2006a). Particle-in-cell simulations of reconnection show that the narrow current layers form at the X-line and produce secondary magnetic islands (Drake et al 2006b) that result in strong electron energization. While some acceleration comes from parallel electric fields, the primary energy gain is due to the contraction of the initially squashed magnetic islands. Electrons circulating rapidly within the islands gain energy through a Fermi process, reflecting off the ends of the islands as they move inward at the Alfvén speed. Up to 60% of the released magnetic energy is transferred to the electrons in the process. The computed energy spectra depend on the plasma β, and agree well with the magnetotail observations (Oieroset et al 2002), while the limiting $\beta = 0$ case produces very flat spectra similar to those observed in the most intense flares.

Further work by the same group (Cassak et al 2006) show how a spontaneous transition from slow Sweet-Parker reconnection (needed to be able to store magnetic energy) to fast magnetic reconnection can occur in the solar corona.

Oieroset, M. et al. 2002, Phys. Rev. Lett. 89, 195001.
Lin, R. P., & H. S. Hudson, 1971, Solar Phys., 17, 412.
Drake, J.F., et al.2006a, Nature, 443, 553.
Drake,J.F., et al.2006b, Geophys. Res. Lett. 33,L13105
Cassak, P.a. et al. 2006, Ap.J.644, L145.

2.1.1.5 Partially Disk-occulted Flares

Initial RHESSI results (Krucker & Lin 2008) of 55 partially disk-occulted flares reveal that 90% show two components in the HXR range - thermal emission at lower energies and additional emission extending to higher energies with fast time variations and a soft spectrum. Krucker & Lin (2008) suggest that, at least in some events, the rapidly-varying component could be produced in the thin-target scenario (i.e. faint HXR production without significant collisional energy losses) by the same population of electrons that later precipitate and lose their energy by collisions in loop footpoints (thick target).

A typical example is shown in the left panels of fig. 2.1.1-2, where thermal emission originates from a simple loop at the western limb. Above 18 keV, faint nonthermal emission with fast time variations (of the order of tens of seconds) is seen that comes from a loop ~2000 km above the thermal loop observed at the same time. However, the nonthermal loop agrees well in altitude with the thermal flare loop seen later, at the time of the soft X-ray peak. This is consistent with simple flare models (from Krucker et al. 2007).

The right panels of fig. 2.1.1-2 show a rare example where the nonthermal emission originates clearly from above the thermal flare loops (~8000 km above in this case), similar to the Masuda flare (Masuda et al. 1994). However, later in this event, the thermal loops never reach the altitude of the nonthermal source.

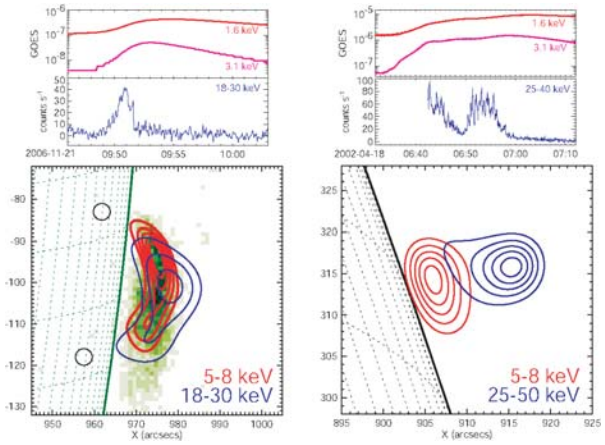

Fig. 2.1.1-2. Two examples of RHESSI X-ray observations of partially occulted flares. Top panels: GOES soft X-ray (red) and RHESSI hard X-ray (blue) time profiles. Bottom panels: RHESSI imaging results with thermal emission in red and nonthermal emission in blue.

Within the next few years, we expect that there will be many joint observations of flares that will be disk-occulted from RHESSI and Hinode/XRT but that one of the STEREO spacecraft will see on the disk. Thus, RHESSI and Hinode/XRT observations will provide imaging of thermal coronal emissions at different temperatures (first results were published by Krucker et al. 2007), while one of the STEREO spacecraft will show the full flare geometry including the location of EUV ribbons. This will place the coronal HXR emission in the context of the flare ribbons.

Masuda et al., Nature, 371, 495, 1994.
Krucker, S.; Lin, R. P., ApJ, 673, 1181, 2008.

2.1.1.6 Hard X-ray emissions from the high corona associated with CMEs

For flares occurring 20 or more degrees behind the solar limb, not only the HXR footpoints but also the main thermal and nonthermal HXR emissions from the corona are occulted, and flare-related emissions from the high corona (>200 arcsec above the flare site) can be seen. Krucker et al. (2007a) found evidence that all fast (>1500 km s^{-1}) farside CMEs that originated from flares occulted by 20° to 45° may show related HXR emissions from the high corona.

RHESSI provides the first high-resolution imaging spectroscopy of HXR emission from such sources (Fig. 2.1.1-3 & 4). The first RHESSI observations analyzed show large sources (>200 arcsec) that expand and move outwards. The speed of the hard X-ray source is lower than the speed of the CME front, but similar to the speed of the trailing filament. This suggests that energetic electrons are being advected outwards in magnetic flux tubes related to the CME.

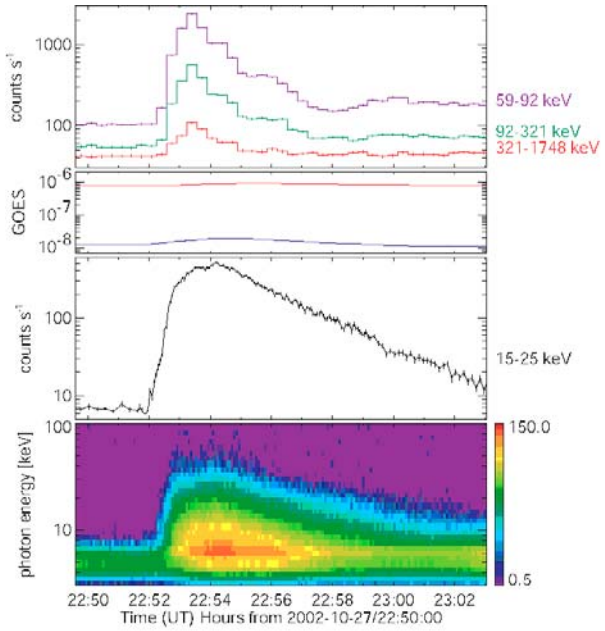

Fig. 2.1.1-3. Time profile of the October 27, 2002 event that was seen on-disk from Mars, while for Earth-orbiting spacecraft the flare site was occulted by at least 200 arcsec (0.2 solar radius). From top to bottom the panels show, (1) GRS X-ray and gamma-ray time profiles seen from Mars (entire flare is seen), (2) GOES soft X-ray flux seen from Earth, (3) RHESSI 15-25 keV time profile seen from Earth, (4) RHESSI HXR spectrogram.

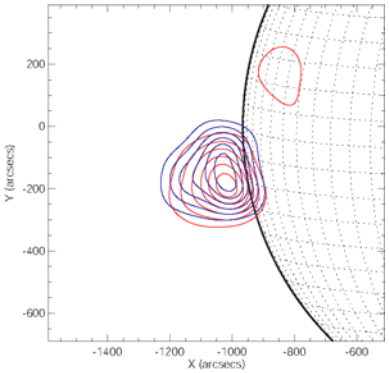

Fig. 2.1.1-4. RHESSI X-ray imaging in the thermal range (3-7 keV, red contours) and nonthermal range (10-30 keV, blue contours) reveal large sources (>200 arcsec) seen just above the limb. The RHESSI CLEAN algorithm was used to reconstruct these images, and the contour levels are at 15, 30, 45, 60, 75, and 90% of the maximum. The thermal emission on the disk around -800/200 arcsec is from AR10717 and was already present before the flare started.

Multi-spacecraft observations had already shown that such HXR emissions from the high corona could occur during the impulsive phase of the flare, simultaneously with the HXR footpoint emissions. The

time profiles of the high coronal events all look similar and show a relatively simple time evolution, with a fast rise and a slower exponential decay. The exponential decay is surprisingly constant, lasting sometimes several minutes without significant deviation, and the photon spectrum exhibits progressive spectral hardening. This might indicate that collisional losses dominate without further acceleration. The relatively simple spectral shape and temporal evolution of these events simplifies spectral inversion and the direct determination of the spectrum of the accelerated electrons.

2.1.1.7 HXR Source Motions Along Loops

In addition to looptop and above-the-looptop sources and their motions, RHESSI has observed X-ray source motions along the legs of flare loops (Sui et al. 2006, Liu et al. 2006). Sui et al. observed a source region move downward from the top of a flare loop to the footpoints and then back up to the looptop during the duration of a flare. They argue that this motion is partially explained by the soft-hard-soft evolution of the accelerated electron distribution and note that this X-ray source motion can be used to deduce the evolution of the plasma density in the legs of the flare loop. Liu et al. observed upward X-ray source motion in a flare loop and used this motion to deduce the evolution of chromospheric evaporation in the loop.

We expect a dramatic increase in our understanding of coronal hard X-ray sources with the advent of Hinode and STEREO. With STEREO observations, we will often be able to tie down a limb-flare location unambiguously. There also may be improved knowledge of the magnetic structure. This will greatly enhance our understanding of the event geometry. Hinode will also be making coronal observations with its high-resolution soft X-ray telescope and with its EUV imaging spectrograph. For CME-related events, we will have the opportunity to locate the coronal hard X-ray sources (with their information about the acceleration and the energy release) in the evolving magnetic structure of the eruption for the first time.

Asai, A., Nakajima, H., Shimojo, M., White, S. M., Hudson, H. S., and Lin, R. P. 2006, PASJ, 58, L1

Lin, R.P. and 12 coauthors, ApJL, 595, L69 (2003a).

Lin, R.P. Krucker, S., Holman, G. D., Sui, L., Hurford, G. J., and Schwartz, R. A., Proc. 28th Int. Cosmic Ray Conf., p. 3207 (2003b).

Liu, W., Liu, S.; Jiang, Yan W.; Petrosian, V. 2006, ApJ, 649, 1124.

Masuda, S., Kosugi, T., Hara, H., Tsuneta, S., Ogawara, Y., Nature, 371, 495 (1994).

Qiu, J., Lee, J., and Gary, D. E., ApJ 603, 335 (2004).

Sui, L., Holman, G. D., and Dennis, B. R. 2006, ApJ, 645, L157.

Veronig, A.M., and Brown, J.C., ApJ. 603, L117 (2004).

White, S.M., Krucker, Sam, Shibasaki, K., Yokoyama, T., Shimojo, M., and Kundu, M.R., ApJL, 595, L111 (2003).

2.1.2 Gamma-Rays

Gamma rays are produced when electrons and ions above several hundred keV interact with the solar atmosphere. The gamma-ray spectrum observed from 200 keV to 8.5 MeV by RHESSI during the 20 January 2005 flare is plotted in Figure 2.1.2-3.

2.1.2.1 Gamma-ray-line Imaging

Gamma-ray imaging provides the only available observational technique for studying the spatial distribution of accelerated ions near the Sun. RHESSI is the only instrument available for acquiring such images. The first gamma-ray image of a solar flare was obtained using the intense neutron-capture line at 2.2 MeV in the X4.8 flare of 2002 July 23 (Hurford et al., 2003). Since that event, four more flares have been imaged in the neutron-capture line. For all of these events, most if not all of the gamma-ray line emission came from compact sources in the flare region.

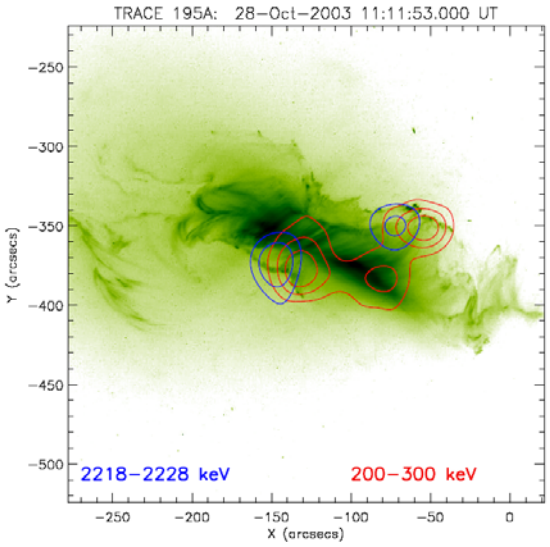

Figure 2.1.2-1. Imaging of the 2.223 MeV neutron-capture line (blue contours) and the HXR electron bremsstrahlung (red contours) of the flare on October 28, 2003. The underlying image is from TRACE at 195 Å. The HXR and γ-ray line double footpoint sources are separated by ~10,000km. Note the apparent loop-top source in the hard X-ray contours.

The, 2003 October 28 flare showed a double source at 2.2 MeV straddling the EUV arcade (Figure 2.1.2-1, Hurford et al, 2006), similar to the HXR footpoints. This is as expected if the ion acceleration is

related to magnetic reconnection, and thus strongly suggests that the parent ions are accelerated in the flare process and not by CME shocks. The gamma-ray line sources are displaced by 10-15 thousand km from the HXR sources for the 2002 July 23 and 2003 Oct 28 flares. At present there is no convincing explanation for this separation.

Hurford, G. J., Schwartz, R. A., Krucker, S., Lin, R. P., Smith, D. M., and Vilmer, N., 2003, ApJ, 595, L77.
Hurford, G. J., et al. 2006, ApJ. 644, L93.

2.1.2.2 Coronal Gamma-ray Continuum Sources

RHESSI provides imaging above 100 keV for the first time, so we now have direct diagnostics of non-thermal electron bremsstrahlung of relativistic flare electrons. Imaging at these high energies is limited by counting statistics, and only the largest flares have high enough counting rates for imaging. So far, only the three events with best counting statistics have been analyzed for coronal emission at the highest energies (Krucker et al., 2008). These reveal, besides footpoint sources, the existence of coronal gamma-ray sources with very hard spectra. For the usual power-law fit to the spectrum, we find indices between 1.5 and 2, suggesting that >1 MeV electrons confined in the corona produce these emissions (Figure 2.1.2-2).

2.1.2.3 Polarization of Gamma-ray Continuum

Boggs et al (2006) and Suarez-Garcia et al. (2006) have reported on the first measurements by RHESSI of the polarization of ~100 –350 keV solar flare gamma-ray continuum produced by near-relativistic electrons. Such polarization would be expected if the parent electrons are beamed, and the direction of polarization is related to the direction of the beaming. The polarization is measured by looking for photons that Compton scatter from one RHESSI detector to another. Since every energy loss is recorded with its time to a microsecond, it is straightforward to search for coincident energy losses in two detectors and determine the direction between the detectors. Systematic errors are reduced since RHESSI rotates rapidly (4s period). The six X-class and one M-class flare range from 0 to ~50% polarization, highly intriguing but only a 2σ result.

Boggs et al. 2006, Ap.J., 638,1129-1139.

Suarez-Garcia et al. 2006, Solar Phys.,239,149.

2.1.2.4 Harder Flare-Accelerated Ion Spectra?

During Solar Cycles 21 and 22, gamma-ray observations made by spectrometers on SMM, Yohkoh, and CGRO indicated that flare-accelerated ions could be represented as power laws with indices ranging from ~3 to ~5. In contrast, four of the best-studied RHESSI flares appeared to have indices ranging from ~2.2 to 3.5 based on early spectral studies. The hardness of the RHESSI flare spectra was inferred from diagnostic line ratios, e.g. Ne/O line ratios, and from the relative weakness of these lines compared to the continuum.

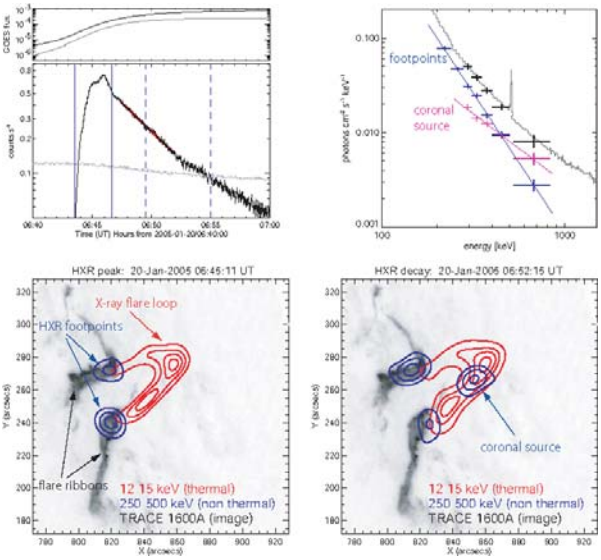

Figure 2.1.2-2. (Top left) Time profiles in GOES soft X-rays and RHESSI gamma-rays for the flare of January 20, 2005. The red line is an exponential fit to the 250-450 keV count rate with a decay time of 257 ± 2s. The vertical lines mark the time intervals of the two images shown below. **(Bottom)** Imaging during the gamma-ray peak **(left)** and the decay **(right).** .Both figures show a TRACE 1600Å image taken at 06:45:11 UT overplotted with 12-15 keV (red) and 250-500 keV (blue) contours. During the peak, the gamma-ray emission is localized at the footpoints, while later an additional coronal source becomes visible. **(Top Right)** Imaging spectroscopy results averaged between 06:46:44 and 06:55:01 UT: The spectrum of the coronal source and the combined footpoint sources are given in magenta and blue, respectively. The power-law fits give a much harder spectrum for the coronal source (gamma = 1.5 ± 0.2) than for the footpoints (gamma = 2.9 ± 0.1). For comparison, the spatially integrated spectrum (gray) and the sum of the coronal and footpoint emission (black) are also shown.

One of the hardest spectra for solar energetic particles (SEPs) ever seen in space was measured during the 2005 January 20 solar flare. The RHESSI gamma-ray spectrum shown in fig. 2.1.2-3 is dominated by the 511-keV annihilation line and the 2.223 MeV neutron-capture line, and by strong bremsstrahlung and nuclear continua. The nuclear de-excitation lines are not prominent. The strong annihilation line was in part due to >20 MeV solar photons interacting in the material surrounding the detectors. The time histories of the different

components of the gamma-ray spectrum are plotted in Fig. 2.1.2-4.

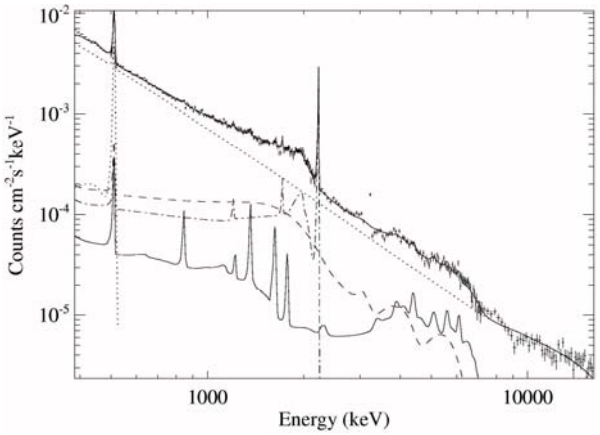

Figure 2.1.2-3. RHESSI gamma-ray spectrum for the 2005 January 20 gamma-ray line flare showing the different contributions to the count rate spectrum.

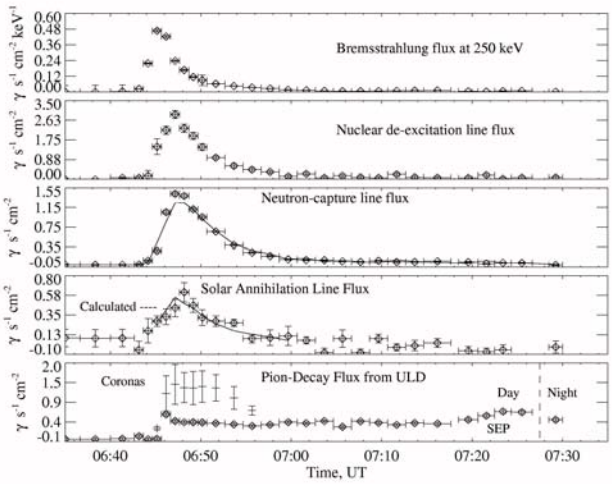

Figure 2.1.2-4. Time history of various gamma-ray components measured by RHESSI during the 2005 January 20 solar flare.

The bremsstrahlung component rises and peaks before the nuclear de-excitation line emission, consistent with what is expected for particle transport in a magnetic loop. The neutron-capture line peaks later due to the slowing down and capture of the neutrons deep in the solar atmosphere. The annihilation line peaks even later due its dominant origin from radioactive decays (a fraction of the line flux comes from positrons arising in pion decays).

A comparison of the various line intensities suggests that the spectrum of accelerated particles is consistent with a power law with an index of ~3. The bottom panel shows the time history of the count rate of pulses that triggered the upper-level-discriminator set at 20 MeV. It rises much more sharply and lasts longer than any of the lower-energy components. As we show in a later section, this high-energy emission (>20 MeV) appears to have been detected into the next RHESSI orbit. We attribute it to the decay of charged and neutral pions produced by >300 MeV protons (this is confirmed by Coronas SONG measurements). The spectrum of accelerated particles producing the pion-decay radiation appears to be a distinctly different component having a significantly harder spectrum than the normal impulsive component. Some of the conclusions reached in this study may change once the flare is reanalyzed using an improved gamma-ray detector response function. We return to this discussion of SEPs in Section 2.1.3.

2.1.2.5 Correlated Electron and Ion Acceleration

We have found a remarkably tight linear correlation ($r^2 = 0.92$) between the 2.223 MeV neutron-capture line fluence and >300 keV bremsstrahlung fluence (Fig, 2.1.2-5) extending over more than three orders of magnitude, taking all RHESSI flares with complete coverage and correcting for limb darkening for the 2.223 MeV line (Shih et al. 2008).

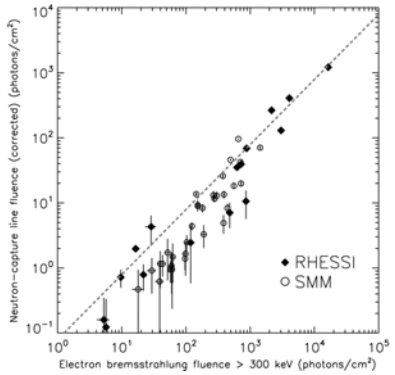

Figure 2.1.2-5 Correlation plot between neutron-capture line fluence and the >300 keV bremsstrahlung fluence for the flares that satisfy the selection criteria (RHESSI in solid diamonds, SMM in hollow circles). The dotted line indicates the best-fit line in linear space that passes through the origin giving a line/continuum ratio of 0.067.

These emissions are produced by >~30 MeV accelerated ions and >300 keV accelerated electrons, respectively. The correlation fits to a straight line passing through the origin, with a ratio of the fluences of 0.067. The individual ratios of 14 of the 16 flares lie within a factor of 2 away from the average, taking into account the $\pm 1\sigma$ errors bars. The correlation also agrees with SMM/GRS data when making the same selection cuts on flares. This proportionality implies that the processes in flares that accelerate electrons above 300 keV and ions above 30 MeV are closely related, and that the relative acceleration of these two populations is independent of flare size.

It appears that solar flares accelerate ions to >30 MeV whenever they accelerate >300 keV electrons down to RHESSI's detection limit. RHESSI has observed flares with >300 keV bremsstrahlung emission that lack neutron-capture line emission, but these flares are invariably near the solar limb or over the solar limb, and thus any neutron-capture line emission would have been severely attenuated by the intervening atmosphere. Thus, there does not appear to be a distinct class of electron-dominated flares.

It is important to note that there are many other flares observed by RHESSI with comparably large GOES classes that have both insignificant >300 keV bremsstrahlung and insignificant gamma-ray emission. This difference could indicate that electrons must be accelerated to some minimum energy before ions are accelerated to high energies. Alternatively, flares with soft energy spectra may accelerate many ions, but not to sufficient energies to produce de-excitation lines or the neutron-capture line.

Shih, A. Y., et al., 2008, in preparation.

2.1.2.6 Gamma-ray and radio sub-millimeter observations

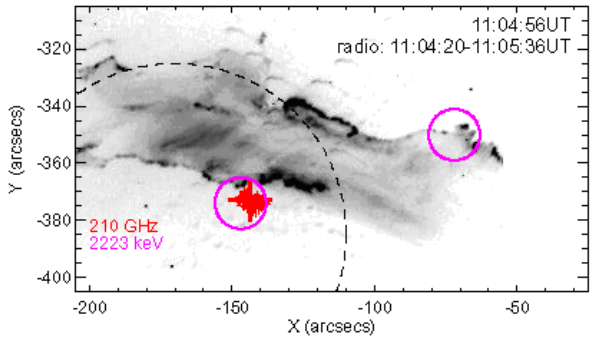

Figure 2.1.2-6. Imaging in radio, UV, and gamma-rays during the October 28, 2003 flare (from Trottet et al. 2008). The TRACE 1600Å image is shown with 210 GHz centroid positions over-plotted as red crosses. The average position and source size of the radio emission is represented by a thick red cross. The dashed circle gives a rough size of the field-of-view of the radio imaging with radio sources outside this circle not represented by the derived source position and size. The thick magenta circles give the flare-averaged 2.2 MeV gamma-ray footpoint locations (from Hurford et al. 2006) with the circle radius representing the 1σ uncertainty in the source location.

The onset of the impulsive component of the radio sub-millimeter emission during the giant flare of October 28, 2003 is simultaneous with the start of high-energy (>200 MeV/nucleon) proton acceleration and the production of pions. The 210 GHz source size is compact (<10 arcsec) and its location is co-spatial with the 2.2 MeV footpoint emission seen by RHESSI (fig. 2.1.2-6). The close correlation in time and space of the sub-millimeter emission with the production of pions suggests that synchrotron emission of positrons produced in charged-pion decay might be responsible for the observed compact radio source. However, order-of-magnitude approximations suggest that the derived number of positrons from charged-pion decay is probably too small. As no spectral information around 210 GHz is available, the emission mechanism of the 210 GHz emission is unclear. A second example of correlated gamma-ray and submm emission is given by Silva et al. (2007) for the 2 Nov. 2003 flare.

Hurford at al., 2006, ApJ 644, L93.
Silva et al. 2007, Solar Phys. 245, 311.
Trottet et al. 2008, in preparation.

2.1.3 HXRs and SEPs

2.1.3.1 RHESSI & WIND Observations

Comparison of Wind measurements of energetic electrons in solar impulsive events with the electrons producing the flare X-ray emission at the Sun observed by RHESSI provides unique information on the energetic electron acceleration and escape processes. For prompt events (where the injection of the electrons at the Sun, inferred from their velocity dispersion, is simultaneous with the X-ray burst) we find that the power-law exponents of the spectra of the electrons at 1 AU and of the X-ray producing electrons are closely correlated, suggesting a common source (Figure 2.1.3-1, Krucker et al., 2007).

However, a simple model, where the electrons observed at 1 AU escape directly from the acceleration source while the downward going accelerated electrons produce the X-rays while losing all their energy to collisions in the dense lower solar atmosphere, does not fit. Some additional acceleration of the downward going electrons may be occurring; if magnetic reconnection does the initial acceleration, possibly the downward going electrons are further accelerated by Fermi and betatron processes as the newly closed field line becomes more dipolar. For several of these events, RHESSI's X-ray imaging together with TRACE imaging of lower temperature plasma, show accompanying jets consistent with reconnection of an open field line with a closed loop (Figure 2.1.3-2).

The spectrum of protons inferred from RHESSI's gamma-ray measurements was found to be very similar to the spectrum of SEP protons observed at 1AU by Wind, ACE, GOES and SAMPEX, for magnetically well-connected flares such as 2 November 2003 and 20 January 2005, suggesting that in those cases some SEPs may indeed come from the flare.

Recent studies show that fast (>1000 km/s) CMEs are accompanied by nonthermal X-ray emission (indicating energetic electrons) detected by RHESSI very high in the corona, but behind the front of the CME. Comparison with energetic electrons accompanying the ICME when it passes Wind will help to resolve the origin of these energetic particles.

2.1.3.2 HXR spectral evolution and SEPs

In a 1995 study, Alan Kiplinger found that flares with HXR spectra that evolved from soft to hard to harder (SHH) are closely associated with high-energy solar proton events observed in interplanetary space. While the physical association between the progressively hardening X-ray spectrum and the particles is not understood at present, the Kiplinger study obtained a 96% success rate in predicting large proton events. If one saw the SHH pattern in HXR spectral evolution, a proton event was almost sure to happen. This association strongly suggests a physical connection between the X-ray-producing electrons in the flare (on the closed flare loops that create the magnetic mirror geometry) and the escaping energetic protons on open field lines. This correlation is puzzling, especially since it is generally believed that an interplanetary shock front, remote from the flare itself, is the main proton accelerator.

RHESSI images show that 20 to 100 keV X-rays originate from footpoints during times with SHH behavior (Figure 2.1.3-3). This was previously noted by Qiu et al. 2004, using Yohkoh/HXT observations of a flare with similar progressive hardening. Hence, if coronal trapping is responsible for the gradual hardening, the hard X-ray emission is not produced by electrons in the corona, but by electrons leaving the trap and precipitating to the footpoints. Therefore, the trapping time in the corona must be shorter than the collisional loss time, at least at energies below ~100 keV. At higher energies (>200 keV), efficient trapping is observed, and, during the decay phase of the HXR burst, coronal emission can even dominate the footpoint emission.

R. Saldanha, S. Krucker, R.P. Lin, ApJ, 673, 1169, 2008

Qiu, J., Lee, J., and Gary, D.E., ApJ, 603, 335, 2004.

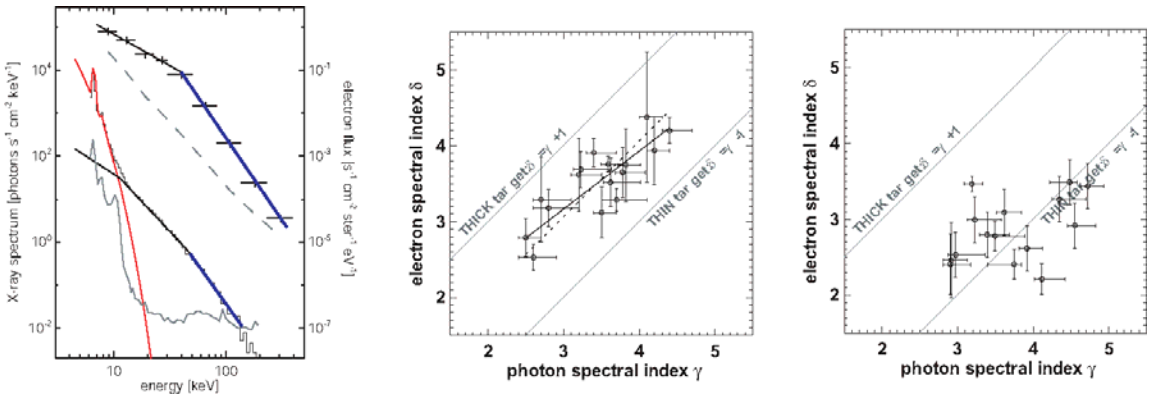

Figure 2.1.3-1. Left: Example of an in-situ electron spectrum and a hard X-ray photon spectrum of a prompt impulsive electron event (April 14, 2002). The top curve shows the in-situ electron peak flux spectrum with the pre-event background spectrum subtracted. A broken power-law fit to the data is shown with spectral indices of -1.5 and -3.9, respectively below and above a break around ~40 keV. The X-ray photon spectrum during the peak of the HXR event is shown below where a thermal (red) and a broken power law are fitted to the data. The thermal component with a temperature of ~14 MK dominates below 12 keV, while at higher energies the spectrum is well represented by a broken power law with spectral indices of 2.8 and 3.4 respectively below and above a break energy of ~48 keV. The gray curves give the pre-event and instrumental background. **Center and Right**: Correlation plot of the photon spectral index γ and electron spectral index δ above ~50 keV for 16 prompt events (middle) and 16 delayed events (right). A positive correlation is found for the prompt events, but no clear dependence is seen for delayed events.

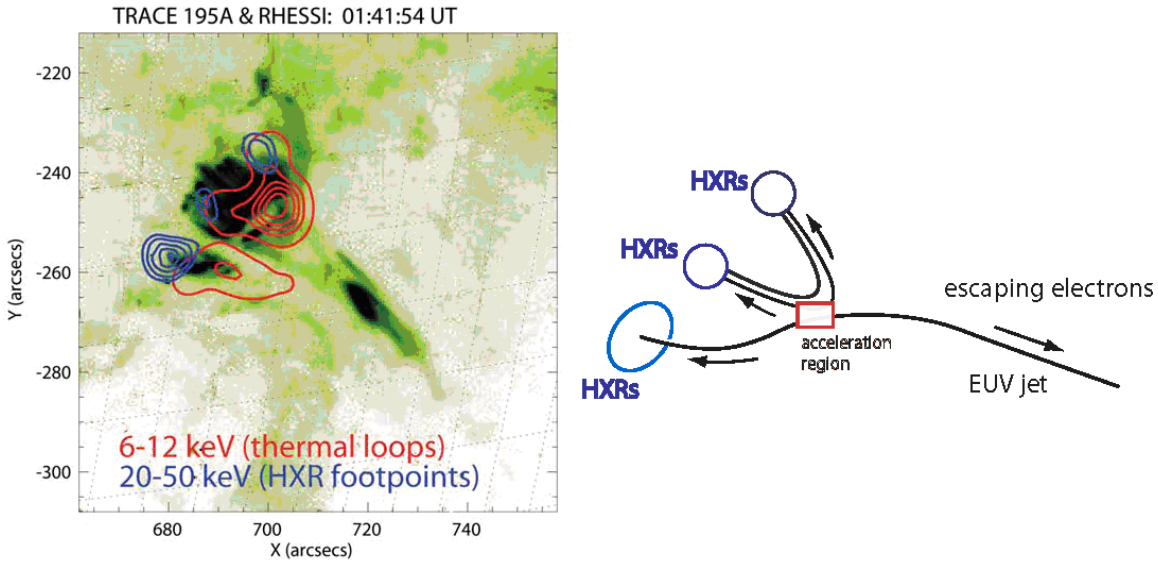

Figure 2.1.3-2. Example of multi-wavelength imaging. **Left:** RHESSI contours at 6-12 keV (red, thermal emission) and 20-50 keV (blue, nonthermal emission) are overlaid on a TRACE 195A~EUV image (dark corresponds to enhanced emission). Around 700/-245 arcsec, the X-ray emission suggests a loop with two nonthermal footpoints.. The strongest nonthermal source, however, is slightly to the south east (683/-257 arcsec) and shows surprisingly a lower intensity thermal source. TRACE observations show an EUV jet at 720,-270 arcsec escaping from the flare region. **Right:** Simple magnetic reconnection models ('interchange reconnection') show similar source structure. The red box marks the reconnection site from where downward moving electrons produce the HXR sources and upward moving electrons escape into interplanetary space.

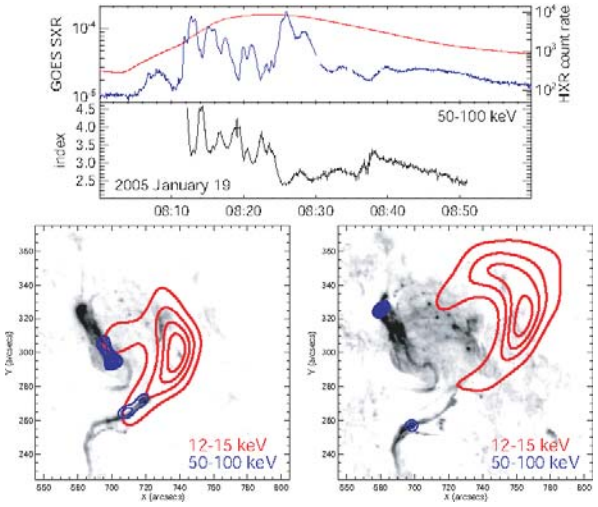

Figure 2.1.3-3. HXR spectral evolution and imaging of the January 19, 2005 X-class flare (Saldanha et al 2008). **Top**. GOES soft X-ray flux (red, low-energy channel) and RHESSI 50-100 keV HXR (blue) count rate. Temporal evolution of the power-law index in the energy range between 50 and 100 keV. **Bottom**. HXR imaging results of the January 19, 2005 flare taken during the first HXR peaks (08:11:40 to 08:13:41 UT, left) with SHS behavior and later during the progressively hardening phase (08:43:10 to 08:45:40 UT, right). Both figures show HXR contours in the thermal (red contours at 20, 40, 60, and 80% of the peak) and nonthermal (blue contours at 7.5, 15, 30, 50, 70, and 90% of the peak) energy ranges superposed on TRACE 1600°Å images taken at 08:25:30 UT (the first image available for this flare) and 08:45:03UT. For both spectral behaviors, soft-hard-soft (SHS) and soft-hard-harder (SHH), non-thermal HXR emissions in the 50-100 keV range are observed from footpoints.

2.1.4 Microflares

2.1.4.1 Microflare Statistics

One proposal for heating the solar atmosphere is via very small flares (microflares, like ordinary flares but weaker, or Parker's "nanoflares") occurring quasi-continuously over the solar disk. The viability of this mechanism depends on the integrated energy of these events and on their ubiquity, particularly in the absence of sunspots. Their integrated energy depends on two factors: their frequency and the low-energy cutoff to the steep nonthermal electron spectrum, which RHESSI has shown dominates the energetics of the weakest events (Krucker et al., 2002). RHESSI has high sensitivity (to detect the smallest events), spectral resolution and coverage to characterize nonthermal and thermal spectra, and imaging to associate individual microflares with active regions.

RHESSI results (Benz and Grigis 2002, Krucker et al. 2002, Qui et al., Liu et al. 2004, Battaglia et al. 2005, Hannah et al. 2008a) have shown that microflares have relatively steep power-law (viz. nonthermal) spectra extending down to below 10 keV in some cases. This has extended the low-energy cutoff well below that available with previous instruments, a result which has significantly raised estimates of their integrated energy.

Christe et al. (2008) and Hannah et al (2008b) describe a sample of ~25,000 events observed over RHESSI's first five years. Figure 2.1.4-1 shows this sample distributed in approximate heliographic coordinates. There is a strong preference for the microflares in this figure to occur in active regions. They also found that small flares are not necessarily spatially small, with no correlation between the observed thermal loop size and flare magnitude. This study characterized the energy content of these small flares, and presented the first thermal energy (shown in Figure 2.1.4-2) and non-thermal power distributions determined with RHESSI. These observations confirm the strong similarity between microflares and "real" flares that are orders of magnitude more energetic. All events with sufficient counts for imaging are found to be located in active regions. They are too intermittent in both space and time to "explain" the heating of the general corona but their total energy is roughly comparable to that needed to support the general corona or the non-flaring active-region loop structures.

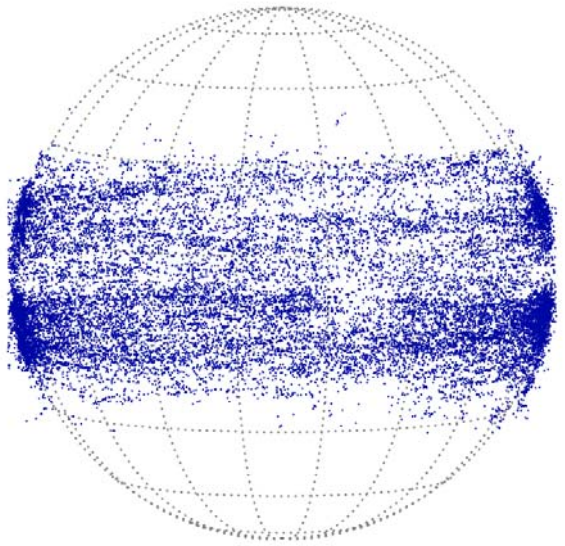

Figure 2.1.4-1. Locations of ~25,000 microflares observed by RHESSI during its first five years of operation from 2002 through to 2007.

The limb events are particularly interesting. A glance at fig. 2.1.4-1 shows that many locations lie just above the limb. (Note that RHESSI's high angular resolution is precise at the sub-arc-second level for centroiding, even for weak events.) Thus, a study analogous to that done by Matsushita et al. (1992) for the much inferior HXT observations needs urgently to be carried out. This and related studies can now be done in the context of the STEREO data, which will greatly help in understanding the geometry (even in 2D, i.e., just for footpoint identification) of limb events seen by RHESSI.

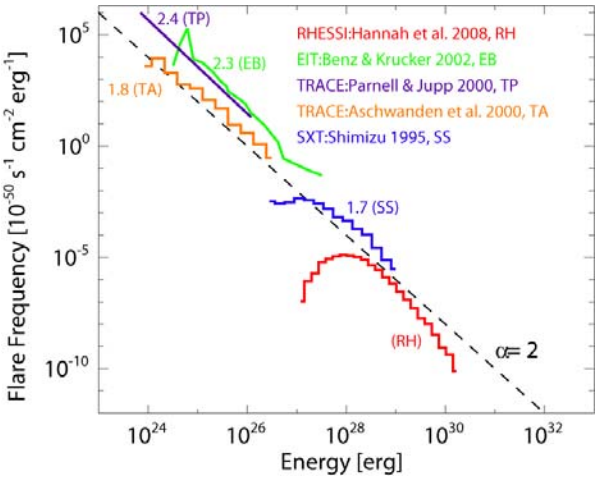

Figure 2.1.4-2 The first RHESSI thermal energy distribution of microflares (Hannah et al. 2008). The peak thermal energy for the RHESSI microflares is shown in comparison to the thermal energy distributions found for soft X-ray active region transient brightenings and EUV nanoflares with EIT and TRACE.

Battaglia, M.; Grigis, P. C.; Benz, A. O., A&A. 439, 737, 2005.

Christe S., Hannah I.G., Krucker S. Lin R.P, McTiernan J, ApJ, 2008, in press.

Hannah I.G., Christe S., Krucker S. Hurford G.J, Hudson H.S, Lin R.P, ApJ 2008a, in press

Hannah I.G., Krucker S., Hudson H.S., Christe S., Lin R.P., A&A 2008b, in press.

Hudson, H. S., Hannah, I. G., DeLuca, E. E., and Weber, M., in Proc. 1st *Hinode* Sci. mtg (2008).

Krucker, S., Christe, S., Lin, R.P., Hurford, G.J., and Schwartz, R.A.; Solar Phys. 210, 445-456, 2002.

Liu, C.; Qiu, J.; Gary, D. E.; Krucker, S.; Wang, H., ApJ 604, 442, 2004.

Matsushita, K., Masuda, S., Kosugi, T., Inda, M., and Yaji, K., Solar Phys. 44, L89 (1992).

Neupert, W., Ann. Rev. Aston. Astophys. 7, 121-148, 1969.

Qiu, J., Liu, C., Gary, D. E., Nita, G. M., Wang, H., ApJ, 612, 530, 2004.

2.1.4.2 Microflares with RHESSI & Hinode/XRT

Individual microflares have been analyzed using both RHESSI and Hinode/XRT. An example is shown in fig. 2.1.4-3. RHESSI provides information regarding the energy content of the accelerated electrons and where this energy is deposited. The high sensitivity and spatial resolution of Hinode/XRT can then be used to observe the dynamic response to this deposited energy. RHESSI is also available to image and provide physical characteristics (through spectroscopy) of the hotter component of the thermal plasma response. This has been done in detail for a single microflare, also using TRACE EUV data in addition to RHESSI and Hinode/XRT, to observe the cooler EUV response (Hannah 2008).

Hannah I.G., Krucker S., Hudson H.S., Christe S., Lin R.P., A&A 2008b, in press.

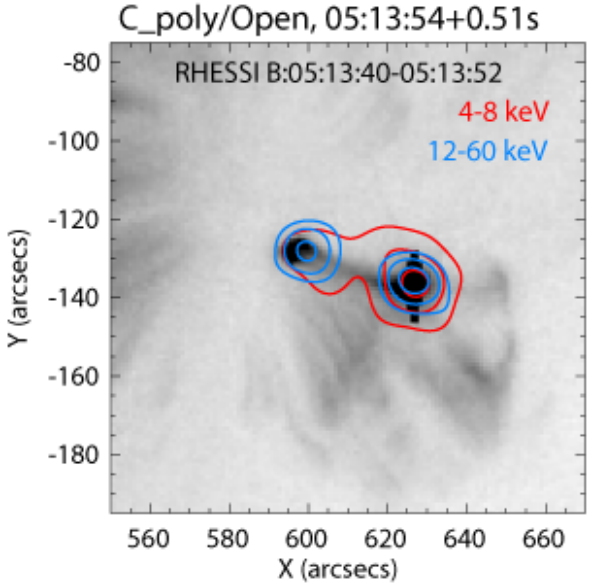

Figure 2.1.4-3 X-ray image from both RHESSI (coloured contours) and Hinode/XRT (background image) (Hannah et al. 2008b). RHESSI shows where the accelerated electrons are depositing their energy (blue contours) and Hinode/XRT the dynamical response of the heated plasma as it fills the post-flare loops.

2.1.5 Quiet-Sun & Axion Observations

RHESSI's design is optimized for flare observations but we have been able to push RHESSI's capabilities to observe fainter solar emission, which we plan to continue through 2008 and 2009. The fan-beam modulation technique (Hannah et al. 2007a) was developed to allow the faint solar disk to be distinguished from instrumental and terrestrial background. It requires pointing RHESSI slightly off the solar disk (between 0.4 and 1˚), thus chopping the solar signal as the spacecraft rotates at ~15 rpm. This off-pointing process has been successfully conducted several times since 2005 during periods of quiet Sun when there have been no active regions/sunspots on the disk. Initial analysis of these observations has produced upper limits to the quiet-Sun X-ray flux between 3 to 200 keV and showed that the 3-6 keV emission from the quiet Sun is at least two orders of magnitude smaller than the smallest microflares observed with RHESSI (Hannah et al. 2007b). This is shown in Figure 2.1.5-1 as well as the fact that the non-flaring sun emission appears to correlate to the softer GOES X-ray emission in a similar manner to microflares, suggesting that there might be an unresolved ensemble of microflares being responsible for this non-active region emission.

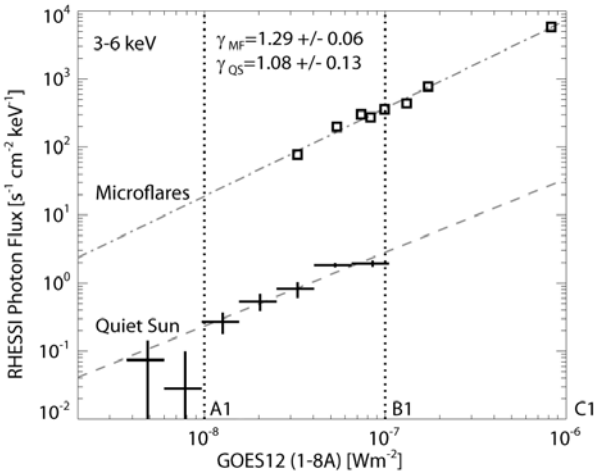

Figure 2.1.5-1. The use of the Fan beam modulation technique (Hannah et al. 2007a) allows RHESSI to observe the non-flaring Sun, finding that the quiet emission is over two orders of magnitude fainter than that in small microflares and that it correlates with the softer GOES observed X-ray emission in a similar way to the microflares (Hannah et al. 2007b).

The limits of the quiet-Sun emission found with RHESSI have been used to put limits on the coupling constant of the theoretical axion particle (Hannah 2007b). These particles have been postulated to solve the strong-CP problem in quantum chromodynamics and have a cosmological significance as a dark-matter candidate. Solar axions should be produced copiously in the Sun's core via nuclear reactions, with the average energy calculated to be 4.2 keV (Van Bibber et al. 1989) and with a narrow ^{57}Fe line near 14 keV (Moriyama 1995). These axions can directly convert to X-ray photons of the same energy in the corona through interactions with magnetic fields perpendicular to their velocity vector. The limits found with RHESSI are comparable to the limits on the axion-photon coupling constant found with the CERN Axion Solar

Telescope (CAST) (Andrianonje et al. 2007) for low mass axions.

Andrianonje et al., J. Cosmology and Astroparticle Phys. JCAP, 04 2007.

Hannah I.G., Hurford G.J, Hudson H.S., Lin R.P., Rev Sci Ins 78, 024501 2007a.

Hannah I.G., Hurford G.J, Hudson H.S., Lin R.P, van Bibber K, ApJL 659 L77 2007b.

Hannah I.G., Hurford G.J, Hudson H.S., Lin R.P, van Bibber K, ApJL 659 L77 2007b.

2.1.6 HXR correlations with CMEs

Given the geoeffectiveness of CMEs, the effort to understand and eventually to predict these powerful solar events has become a major activity of the HD program. As we know, CMEs sometimes occur without flares and vice-versa, but the largest flares tend to be associated with fast and powerful CMEs.

Most models of these events include an intimate magnetic connection between the initiation and early acceleration of the CME and the energy release in the associated flare. Dramatic support for this connection has come from the comparison of the acceleration rate of two CMEs and the HXR light curve seen with RHESSI - see fig. 2.1.6-1 from Temmer et al. (2008). They studied two fast halo CMEs where early signatures of the CME impulsive acceleration phase could be identified in on-disk SXI and TRACE images with high time cadence, and where the impulsive phase of the associated flare was fully covered by RHESSI. Since the flare HXR flux is directly related to the number and energy distribution of accelerated electrons which contain a large fraction of the total flare energy, this data set enabled them to study the relationship between the large-scale CME acceleration and the energy release in the associated flare.

A tight synchronization between the CME acceleration and the flare HXR bursts was found in both cases; onsets as well as peaks occurred simultaneously within about 5 minutes (i.e. within the observational limitations). These findings show a close relationship between the two phenomena, consistent with magnetic reconnection occurring in a current sheet behind the CME, as envisaged in the standard flare/CME picture. On the one hand, magnetic reconnection adds poloidal flux to the CME sustaining the Lorentz force which drives the CME acceleration. On the other hand, the higher the acceleration of the CME, the larger the space that is evacuated per unit time in the coronal region behind it. External magnetic pressure then drives a stronger mass inflow into the reconnection region, which, in turn, causes stronger magnetic reconnection in the current sheet beneath, i.e., stronger flare energy release.

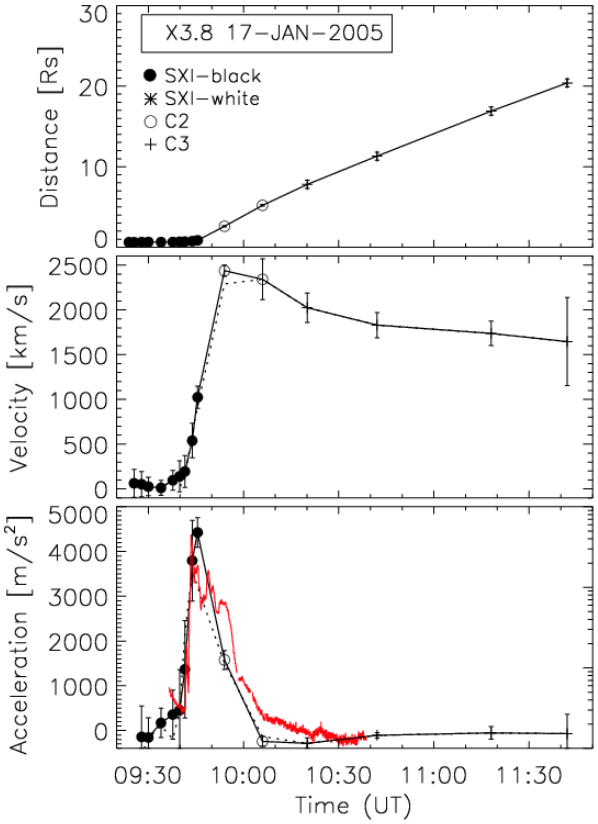

Fig. 2.1.6-1. Event of 2005 January 17. From top to bottom, distance-time profile, d(t), velocity v(t), and acceleration a(t) of the CME as observed by SXI and LASCO-C2 & C3. In the bottom panel, the red line shows the RHESSI 50–100 keV HXR count-rate light curve of the associated flare plotted on a log scale extending from 10 to 10^4 counts s^{-1} detector^{-1}.

In the 2002 April 15 flare, the coronal X-ray source changed its motion within about one minute from being approximately stationary to moving outward at about 300 km s^{-1}. This speed was found to be consistent with that of an associated CME observed later with LASCO. Several weak X-ray sources were later observed along the line of motion of the original coronal source, indicating the continued presence of a current sheet below the CME and the presence of instabilities within the current sheet (Sui et al. 2005). For the homologous flare on 2002 April 16, *SOHO* SUMER spectra combined with RHESSI data have provided evidence for the presence of upward and downward reconnection jets in the above-the-loop-top region (Wang et al. 2007).

Wang, T. et al., ApJ 661L, 207, 2007

Temmer, M. et al., ApJ 673, 95, 2008

2.1.7 Solar Oblateness

The RHESSI system for precise aspect determination includes a Solar Aspect System (SAS) with a simple design but remarkable properties (Fivian et al. 2005). Essentially it follows the idea of Dicke's "Solar oblateness telescope" (Dicke and Goldenberg, 1967) in having sensors on a rotating telescope continually scanning the limb of the Sun. The data are very numerous: about 100 measures per second, each with a statistical error measured at a few *mas* (milli arc sec). Because of RHESSI's ~15 rpm rotation, these data are distributed around the entire limb and are thus an excellent tool for measuring the shape of the Sun and its time variations. We regard this as a new independent window on the structure and dynamics of the solar interior, independent of helioseismology and of the neutrino observations.

The SAS data have recently produced their first result, a measure of the solar oblateness with statistical errors of about 0.1 *mas* (corresponding to less than 100 m in height). At this level of precision many systematic terms need to be considered, and the data reduction scheme – though simple in principle – is quite complex. Accordingly we have only thus far reduced a preliminary 3-month data set as described below. In particular, faculae (and sunspots) produce obvious signatures, as seen in Figure2.1.9-1.

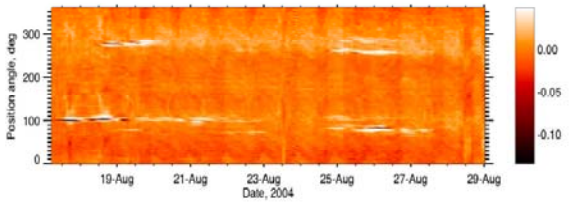

Figure 2.1.9-1. Gray-scale representation of RHESSI radius observations for a two-week interval in 2004, at moderate solar activity. The color bar is calibrated in arcsec. Sunspots are radius deficits, hence dark features; faculae are radius excesses, hence bright features. The rotationally-induced oblateness can be seen as blurred excesses at the W and E limbs (90° and 270°).

Fig. 2.1.9-2 shows a limb profile (the Y-axis of Fig. 2.1.9-1 for selected data), illustrating the great precision of the observations. The novel finding is that there is a large apparent oblateness significantly in excess of that expected from rotational flattening. This is present even for the data selected to omit all apparent faculae, based on synoptic charts such as that of Fig. 2.1.9-1. Fig. 2.1.9-2 (right) shows the four limb quadrants averaged together; the lowest line shows Dicke's (1970) estimate of the rotational flattening.

To make the first oblateness determination, Fivian et al. (2008) use SOHO/EIT observations as a sensitive proxy for faculae, finding a good correlation with RHESSI radius as expected from Figure 2.1.9-1. Using this correlation to identify clean data produces a strikingly different result from that seen in Figure 2.1.9-2: the measured oblateness is now consistent, within errors, with that expected from surface rotation (and helioseismology). This result shows the existence of a general level of facular brightening extended across the disk, evident in EUV observations and also in the RHESSI radius determinations. We believe this to be the "active network" that Leighton-type models of solar surface magnetism describe as magnetic flux diffusing away from decayed sunspot groups. RHESSI has sufficient resolution to avoid these regions and thus to be able to measure the "true" oblateness, i.e. that created by rotation.

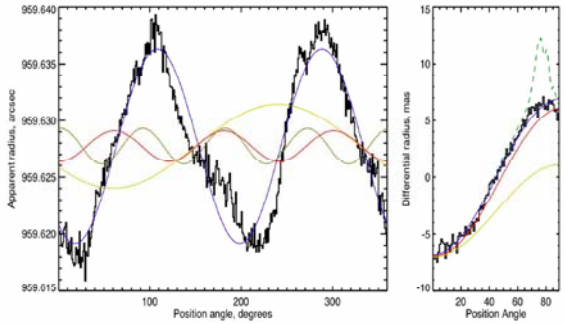

Figure 2.1.9-2. Limb profiles for data selected to avoid faculae. The right-hand plot folds all four quadrants together. The dashed line shows the full data set with its obvious active-region faculae at 70-80˚ co-latitude. The gold line at the bottom of the plot shows Dicke's estimate of rigid-body rotational flattening. RHESSI detects a broad excess oblateness.

Dicke, R. H., and Goldenberg, H. M.: Phys. Rev. Lett. 18, 313, 1967.

Dicke, R. H., 1970, ApJ 159, 1.

Fivian, M.D., Hudson, H.S., and Lin, R.P., 2005, in *Proc. 11th European Solar Physics Meeting*, ESA SP-600, 41.

Fivian, M.D., Hudson, H. S., Lin, R. P., and Zahid, H. J., *Nature* (submitted 2008).

2.1.8 Terrestrial Gamma-ray Flashes (TGFs)

Beginning in 2005 (Smith et al. 2005), RHESSI unexpectedly revitalized the study of Terrestrial Gamma-Ray Flashes (TGFs), and indeed the entire field of high-energy processes in thunderstorms, by detecting over 100 of these events per year. This is greater than the entire previous dataset (75 events) from the Compton Gamma-ray Observatory, the only mission to detect this phenomenon previously (Fishman et al. 1994). All that was known about TGFs prior to 2005 was that they are millisecond bursts of

gamma-rays extending up to ~20 MeV seen above thunderstorms. From analyzing the RHESSI data, we now know the following about TGFs:

- The gamma-ray spectrum shows that they are the result of a process called Relativistic Runaway that accelerates electrons to >~30 MeV in <~1ms (Dwyer and Smith 2005; Carlson et al. 2007);
- Nearly all TGFs can be associated with individual lightning strikes (Cummer et al. 2005; Inan et al. 2006);
- The type of associated lightning is primarily intra-cloud (Stanley et al. 2006; Williams et al. 2006);
- They are primarily produced at altitudes centered around 13-15 km (Dwyer and Smith 2005);
- They also produce beams of electrons up to 30 MeV that sometimes enter the magnetosphere and can be directly seen from orbit (Dwyer et al. 2008; Smith et al. 2008).

Carlson, B. E. et al. 2007, GRL, 34, CiteID L08809
Cummer, S. A. et al. 2005, GRL, 32, CiteID L08811
Dwyer, J. R. and Smith, D. M. 2005, GRL, 32, CiteID L22804
Dwyer, J. R. et al. 2008, accepted to GRL
Inan, U.S. et al. 2006, GRL, 33, CiteID L18802
Fishman, G. J. et al. 1994, Science, 264, 1313
Smith, D. M. 2004, Proc. 5th INTEGRAL Workshop, p. 45
Smith, D. M. et al. 2005, Science, 307, 1085
Smith, D. M. et al. 2008, in preparation for JGR
Williams, E. et al. 2006, JGRD 111, CiteID D16209

2.1.9 Astrophysics Results

2.1.9.1 Gamma-Ray Bursts (GRB's)

Thanks to its broad energy range and wide field of view, RHESSI has made valuable contributions to the study of astrophysical Gamma Ray Bursts (GRBs). These energetic transients have peak energies ranging from tens to hundreds of keV. Determining this peak energy via spectral fitting helps constrain overall burst energetics and may provide information about its intrinsic luminosity via a variety of empirical correlations. The Swift GRB satellite which localizes many bursts is sensitive only to 150 keV, so RHESSI has played a key role in extending spectral coverage of GRBs into the MeV range.

Through July 2007, RHESSI has observed ~420 GRBs, though the majority do not have the localization required for further spectral analysis. Spectral parameters were reported to the community via the GCN Circulars for eight GRBs beginning in 2006. Detailed studies of GRBs 061126 and 070125 were reported by Perley et al. (2007) and Bellm et al. (2007a). Wigger et al. (2008) found a statistically significant high-energy excess in the RHESSI data of GRB 021206, providing support for a specific model of the still poorly-understood GRB emission mechanism. Bellm et al. (2007b) performed joint spectral fits on 26 bursts observed by RHESSI and Swift-BAT.

RHESSI's excellent timing resolution has also made it possible to probe the Quantum Gravity energy scale in the range 10^{16}-10^{19} GeV, up to the Planck mass scale, place limits on quantum gravity effects, manifested as a modification in the electromagnetic radiation dispersion relation, specifically, a (small) energy dependence of the velocity of light. This is seen as energy-dependent delays in GRB pulses. To approach the Planck mass scale, we must measure arrival time differences e.g. of on the order of 0.5 ms from soft to ~10 MeV photons from an event at a redshift of a few. Boggs et al (2004) used GRB 021206 to derive one of the most stringent limits on the quantum gravity energy scale to date. There is a systematic search for millisecond flares in RHESSI GRBs with >1 MeV photons. This work to date is summarized in Wunderer et al (2007).

In December 27, 2004 the known soft gamma-ray repeater SGR 1806-20 underwent a cataclysmic giant flare, the brightest gamma-ray event observed in over 30 years of monitoring the high-energy sky. A series of letters were published in Nature, led by a full article on the RHESSI analysis and results (Hurley et al., 2005). Recently, the comprehensive analysis of the RHESSI (and Wind) observations of this giant flare was published by Boggs et al. (2007).

RHESSI GCN Circulars: 5418, 5685, 5725, 5838, 5867, 6025, 6135, 6399
Bellm, E., et al. 2007a, arXiv:0710.4590
Bellm, E., et al. 2007b, arXiv:0801.2417, to appear in the proceedings of Gamma Ray Bursts 2007
Boggs, S., C. Wunderer, K. Hurley, and W. Coburn 2004, ApJ 611, L77
Boggs, S.E. et al. 2005, ApJ., 611, L77-L80.
Boggs, S., A. Zoglauer, E. Bellm, K. Hurley, R. P. Lin, D. M. Smith, C. Wigger, W. Hajdas 2007, ApJ 661, 458
Hurley et al., 2005, Nature, 434, 109.
Perley, D., et al. 2008, ApJ 672, 449
Wigger, C., et al. 2008, ApJ 675, 553
Wunderer, C., E. Bellm, S. Boggs, and K. Hurley 2007, AIPC 921, 512 O

2.1.9.2 Accreting X-ray binary A0535+26

In May 2005, the accreting X-ray binary A0535+26 underwent a rare (the last outburst was in 1994) and remarkable outburst reaching a brightness several times that of the Crab Nebula. At the time, it was tens of degrees from the Sun, and Swift was only able to observe it briefly because of the solar pointing

constraints, missing most of the outburst. This also prevented any other instrument but RHESSI from observing it. RHESSI was able to take advantage of its off-pointing capabilities to follow this source for several weeks during this outburst. Boggs & Smith (2006) reported on a search in the RHESSI data for a red-shifted neutron-capture (2.223 MeV) line, and obtained the first upper limits for an accreting neutron star source.

2.2 SCIENCE OBJECTIVES for 2008 - 2012

2.2.1 Flare Rates and Energetic Events

We are now very near the minimum in solar activity as indicated in Figure 2.2-1 by the flare rates recorded by different instruments over the last three cycles. In 2009-10, solar activity will be steeply rising again towards the next solar maximum, and RHESSI's high-energy measurements will be essential to the HGO.

Large flares, fast CMEs, and SEP events still occur but are less frequent near solar minimum. Such events are important because of simpler conditions in the coronal and solar wind. STEREO and Hinode were launched in 2006 to join the HGO and the Solar Dynamics Observatory (SDO) will be launched in 2008. RHESSI is the ideal high-energy complement to the high-resolution optical imager and vector magnetograph, soft X-ray imaging, and EUV imaging spectroscopy of Hinode, and the 3-D imaging in EUV and white-light coronagraphy of STEREO for studying flares and CME initiation. STEREO's highly sensitive energetic electron and ion measurements, separated in longitude, are perfect for comparisons with RHESSI's sensitive measurements of energetic particles at the Sun near solar minimum when the background is low. Solar minimum will also enable RHESSI to make deep searches for microflares and quiet-Sun nonthermal emissions.

As pointed out earlier, much work remains to be done to develop methods and software to mine the information in the rich RHESSI data set. In addition we propose a GI program to integrate the remarkable new observations of solar eruptions and their energetic consequences obtained by HGO in the last solar maximum. As always RHESSI will contribute unique measurements for study of Terrestrial Gamma-ray Flashes and cosmic gamma-ray bursts and other high energy astrophysical phenomena.

Figure 2.2-1. Predicted rates of X-ray flares for the next solar cycle (blue curve) based on the average of the rates from the three previous cycles as measured with other X-ray instruments (ISEE-3, SMM/HXRBS, CGRO/BATSE, and Yohkoh/HXT (Aschwanden, private communication). The black histogram shows the rate of GOES >C3 flares, and the measured rates for the other two instruments (Yohkoh/HXT in red and RHESSI in orange) have been normalized to that rate

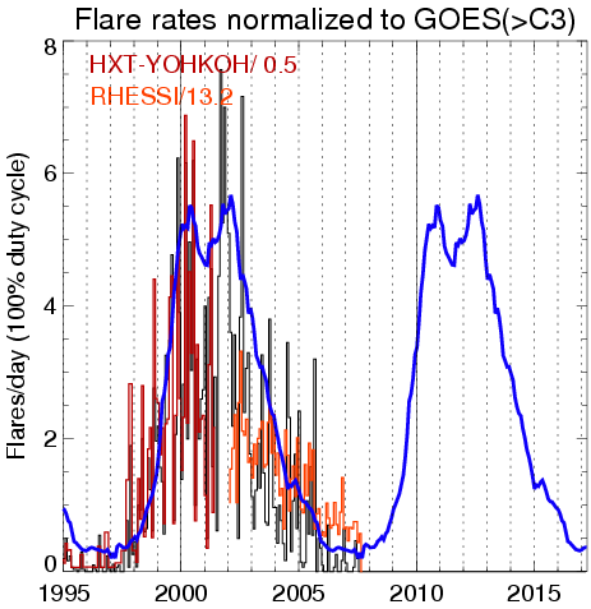

by dividing by the indicated factors.

2.2.2 RHESSI Flare Studies with Hinode and STEREO

Comparing STEREO and Hinode observations with the RHESSI data set will greatly enhance the scientific return for all three missions. Hinode carries a high-resolution optical telescope (SOT), an EUV imaging spectrograph (EIS), and a soft X-ray telescope (XRT), perfect complements to RHESSI's high-energy observations for studies of solar activity. Hinode/SOT will provide the first stable time-series observations of the solar vector magnetic field, at the highest possible angular resolution. Together with Hinode/XRT soft X-ray imaging and Hinode/EIS EUV imaging and spectroscopy, this will give the best information to date regarding the pre-event physical conditions in the solar corona. In some manner not yet understood, these conditions change gradually to a "trigger point", at which time an instability or loss of equilibrium occurs (e.g., Forbes 2000). Arguably the best signs of the initiation are the non-thermal effects, as observed by RHESSI, even in the weakest microflares. The combination of RHESSI and Hinode observations thus will provide our best and most objective determination of the trigger conditions.

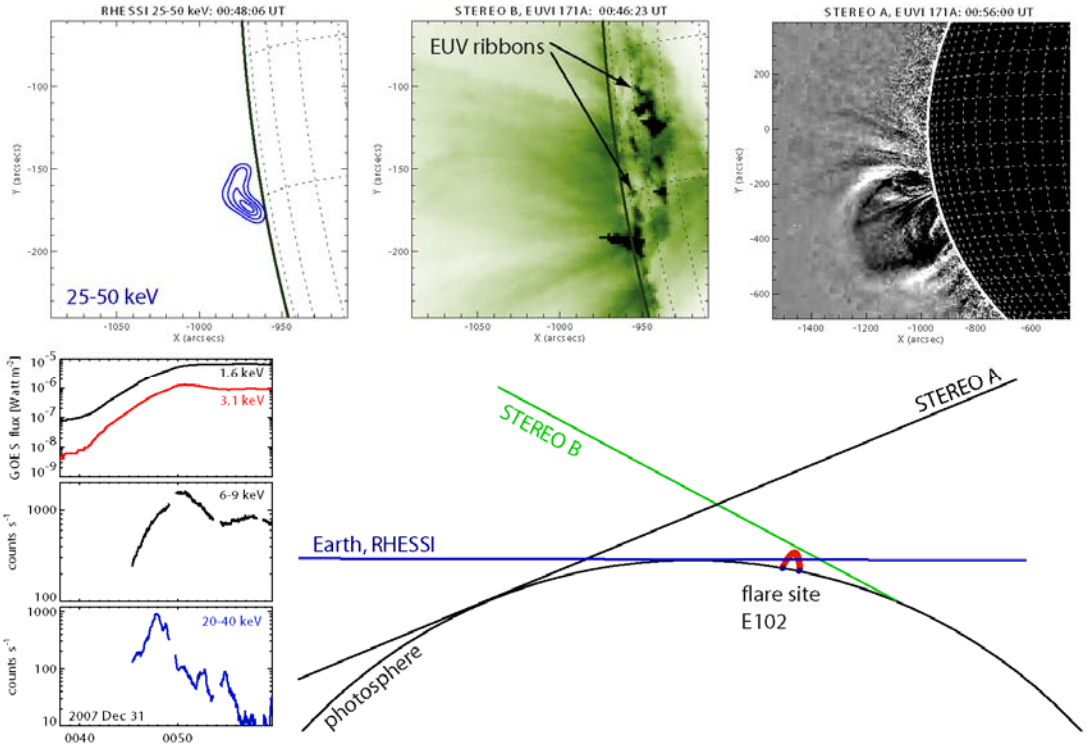

Figure 2.2.2-1. Example of RHESSI-STEREO observations of a partially disk-occulted flare from Earth view seen on December 31, 2007. The cartoon at the bottom right gives the different view angles (to scale). The X-ray time profiles from GOES and RHESSI are shown to the left revealing intense non-thermal emissions above 20 keV. Imaging results are presented in the three figures shown at the top. STEREO/EUVI shows two flare ribbons in north-south direction. The RHESSI source originates most likely from above the loop arcade connecting the EUV ribbons. About 10 minutes later, STEREO A shows the escaping Coronal Mass Ejection (preliminary results).

RHESSI can identify the coronal regions, both pre-flare and during the impulsive phase, that appear to be the sites of flare energy release, magnetic reconnection, and electron (and ion) acceleration. XRT will provide the high-cadence high-resolution imaging of these high-temperature regions (not presently available). RHESSI footpoint motions (Krucker et al., 2003) give a clear indication of the reconnection process in the evolution of the coronal magnetic field. EIS imaging spectroscopy can provide the key measurements of flows and turbulence in these regions to clarify the energy release and particle acceleration processes.

STEREO/EUVI will provide 3-dimensional observations of flare loops seen in EUV. Although RHESSI HXR observations only provide 2-dimensional information, HXR footpoints occur at high density in the chromosphere. Hence, the HXR footpoints can be relatively easily compared with the 3-dimensional geometry obtained from STEREO. Furthermore, Hinode/XRT and RHESSI will provide thermal flare energy estimates, Hinode/EIS will give flow measurements. Hinode vector magnetograms are the first from space, and have high resolution. The development of more accurate coronal field models is a major Hinode objective. The results of this work will allow the field evolution during a flare to be modeled so that different flare models can be compared. RHESSI will provide both thermal and non-thermal electron diagnostics.

STEREO observation will provide different view angles of partially occulted flares seen by RHESSI. For one of the two STEREO spacecraft, the flare will not be occulted, thus providing information about the magnetic structure. This will greatly enhance our understanding of the event geometry. EUV ribbons will give us the likely location of the occulted HXR footpoints. The CME geometry seen with STEREO coronagraphs COR-1/2 can be compared with the HXR coronal source location. RHESSI observations confirm that about 10% of all flares are usefully occulted, i.e. their bright footpoints obscured from view. However, relatively large flares are needed to get good counting statistics so it is expected that only a few good candidates will occur until the flare rate increases

leading up to the next solar maximum. One early example of this situation has already occurred and the preliminary results are shown in fig. 2.2.2-1.

Forbes, T., JGR 105, 23,253 (2000).
Krucker, S., Hurford, G.J., and Lin, R.P., ApJ 595, L103 (2003).

2.2.3 *In Situ* Particle Observations and HXR Emission

For the large flares/SEP events that occur in 2007-8, RHESSI's gamma-ray line measurements of the spectrum of energetic protons and its imaging of the ion source at the Sun can be compared to the ACE, Wind, and STEREO multi-point SEP spectral measurements spread in longitude, while Ulysses will be measuring SEPs when crossing the ecliptic plane at ~1.5 AU. These comparisons could determine whether solar flares directly contribute to SEPs at 1 AU when the flare is magnetically well connected, as suggested by the 2 Nov 03 and 20 Jan 05 events (Section 2.1.4).

Most of the impulsive electron events detected at 1 AU during solar minimum will be seen only below ~15 keV. The excellent sensitivity of RHESSI in the 3-15 keV energy range will give us by far the best chance ever (with two orders of magnitude better sensitivity) to see related HXRs from these events, possibly even the thin-target emission from the escaping electron beams that produce type III radio bursts. Solar minimum conditions with little thermal emission from the corona are optimal for these observations. STEREO will provide 3-dimensional event geometry of the solar source region of the escaping electrons and STEREO/WAVES will track escaping electrons by their radio emission. Although the RHESSI observations are only 2-dimensional images, the relatively simple source structure in X-rays (footpoints) will make it possible to put the X-ray emission in the 3-dimensional geometry.

The STEREO IMPACT suite SupraThermal Electron (STE) and Solar Electron Proton Telscopes (SEPT) instruments will measure impulsive electron events from ~2 to 300 keV. The two STEREO spacecraft will provide these *in situ* measurements at widely separated solar longitudes. By tracking the electrons from the solar source HXR emission imaged by RHESSI, through the interplanetary medium through the Type III radio emission, to the *in situ* detection by the STEREO spacecraft we can trace and study the magnetic connectivity from the Sun to the Earth.

2.2.4 Microflares

Combined microflare observation of RHESSI, STEREO, and Hinode will allow detailed studies of single microflare events to see if microflares are indeed just smaller version of large flares or whether they are a separate type of event. Hinode/EIS will provide observations of plasma flows, while Hinode/SOT, XRT, and EUVI will provide 3-dimensional magnetic structure and estimates of flare volumes. RHESSI observations will be an essential part of these studies since it is the only instrument that can provide higher temperature (>20 MK) diagnostics and give quantitative measurements of the energy content in non-thermal electrons. The energetics of small-scale energy release in the solar atmosphere (microflares, "blinkers", flaring bright points, and many other manifestations) may have a strong relationship to the coronal heating problem.

Individual microflares have begun to be analyzed using both RHESSI and Hinode/XRT (Section.2.1.4..2). The next stage is to investigate statistically the properties of microflares observed with RHESSI and Hinode/XRT. This might also help understand the results of the large RHESSI microflare statistics study (Christe et al. 2008, Hannah et al. 2008).

2.2.5 Quiet-Sun & Axion Observations

RHESSI's recent anneal has lowered the detector background compared to previous offpointing periods and so we hope to improve these quiet-Sun limits further with future offpointings through 2008 and 2009. In addition, we can make use of the softer X-ray observations from Hinode/XRT, whose sensitivity and spatial resolution allow for the detection of bright points across the quiet solar disk. We will investigate if there is a hard X-ray counterpart to these soft X-ray bright points.

We plan to search for the sharp ^{57}Fe line feature in the axion spectrum (Moriyama 1995), which will be easier post-anneal with RHESSI's recovered spatial resolution and suppressed background. We can also exploit the predicted spatial and spectral properties for solar axions to improve on the limits previously found with RHESSI.

Andrianonje et al., J. Cosmology and Astroparticle Phys. JCAP, 04 2007.
Christe S., Hannah I.G., Krucker S. Lin R.P, McTiernan J, ApJ 2008 in press.
Hannah I.G., Hurford G.J, Hudson H.S., Lin R.P., Rev Sci Ins 78, 024501 2007a.
Hannah I.G., Hurford G.J, Hudson H.S., Lin R.P, van Bibber K, ApJL 659 L77 2007b.
Hannah I.G., Christe S. , Krucker S. Hurford G.J, Hudson H.S, Lin R.P, ApJ 2008 in press.
Moriyama S., Phys. Rev. Lett., 75, 3222, 1995.

2.2.6 Gamma-Ray Observations

Future work to improve the reconstructed gamma-ray images will be directed along two lines. First, improved analysis techniques based on ***visibilities*** will improve the statistical significance of the results. Second, improved background- and continuum-subtraction techniques (also visibility-based) represent a promising avenue to permit imaging in the 511 keV line. The significance of this is that RHESSI can image such lower energy gamma-ray line photons with significantly better angular resolution as the finer and thinner grids give usable modulation at this energy.

Of course, as solar maximum approaches, more gamma-ray flares will be detected, allowing more systematic studies.

2.2.6.1 Coordination with GLAST

As early as May 2008, RHESSI will be joined in orbit by the Gamma-ray Large Area Space Telescope (GLAST), providing a unique opportunity to make simultaneous nuclear-line and high-energy (up to several GeV) gamma-ray observations. GLAST will also detect neutral pions produced in the same reactions as the positive pions that yield positrons responsible for the annihilation line observed by RHESSI. The high-energy protons can penetrate below the photosphere and may be responsible for the helioseismic waves and recent near-IR observations. Joint high-sensitivity RHESSI and GLAST measurements also may detect gamma-rays from delayed CME shock-accelerated particles that may impact the solar atmosphere after the impulsive phase of a flare. Delayed annihilation and neutron-capture line emissions have been detected by RHESSI following the impulsive HXR phase of the 10 September 2005 flare.

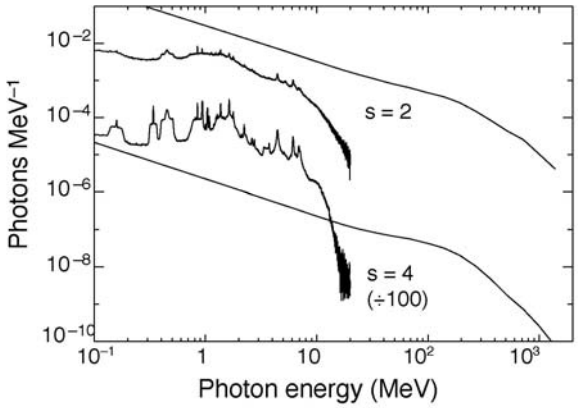

Figure 2.2.6-1. Comparison of nuclear line and pion decay emissions for two flare spectra.

Figure 2.2.6-1 shows how joint RHESSI and GLAST gamma-ray spectral observations can be used to determine the spectrum of flare-accelerated particles. The nuclear-line spectra and the continuum produced by the decay of neutral and charged pions are plotted for two different power-law spectra of flare-accelerated particles. The nuclear-line spectrum dominates over the high-energy continuum for particle with indices steeper than about 3; for harder particle spectra, the continuum dominates. The photon spectrum at energies >1 GeV directly reflects the flare proton spectrum. Joint RHESSI and GLAST observations will allow the pion-decay gamma-ray continuum to be distinguished from the primary electron bremsstrahlung.

High-energy radiation from the 1991 June 11 flare was observed by EGRET and COMPTEL on CGRO for several hours suggesting continued acceleration and/or long-term trapping. *RHESSI* observations of >17 MeV emission indicate that high-energy interactions also occurred in the solar atmosphere for at least two hours following the impulsive phase of the 2005 January 20 flare. The *RHESSI* image of this flare plotted in Figure 2.2.6-3 reveals two hard X-ray footpoints (contours) lying in two ribbons revealed by UV images made by *TRACE*. The centroid of radiation from the 2.223 MeV neutron capture line is identified by the thick white circle about ten arcsec to the E/SE of the peak in hard X-rays in the northern footpoint. For comparison we also show the ~30 arcsec position uncertainty of the LAT for >500 MeV pion-decay photons. Thus, the combined RHESSI/GLAST observations will be able to determine whether high-energy protons also were contained within the closed magnetic loops ending in the footpoints.

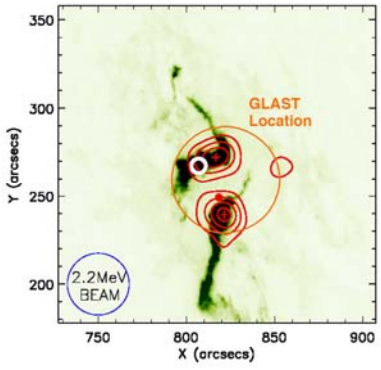

Fig. 2.2.6-3. Red circle shows expected accuracy of LAT location of a 500-MeV source compared with RHESSI 250 – 500 keV contours (in red) and centroid location of the 2.2 MeV emission (white circle) superimposed on a TRACE 1600 Å image (green and black) of the 2005 January 20 flare. The RHESSI beam size at 2.2 MeV is shown as the blue circle.

2.2.7 Solar Limb Data

The RHESSI SAS data extend now for six full years but we hope eventually for the full orbital lifetime of the satellite. They offer a unique resource for a variety of investigations (Table 2.2.7-1), probably the most important (and hardest) being the detection of g-modes. There is some hope that this is possible since the limb is elevated above the photosphere resulting in larger amplitudes. Note that there are g-modes with periods of hours, and so the RHESSI window function (eclipses in low-Earth orbit with a 95-min. period) will not interfere with an analysis of data that spans many years. In general, the longer the data run, the better the signal-to-noise ratio. This unique data set is unlikely to be reproduced and may justify the operation of RHESSI even if its primary mission came to an end.

Table 2.2.7-1: Phenomena accessible with precise radius measurements

Magnetic Phenomena	**Hydrodynamic Phenomena**
sunspots	p-modes
Wilson depression	g-modes
faculae	r-modes ?
active network	granulation
Flares	other convective motions
prominences	oblateness
coronal holes ?	oblateness time variations ?
Dynamo signatures ?	Higher order shape terms
	Gravitational moments J2, J4
	Global temperature variation ?
	Planetary tides

2.2.8 Terrestrial Gamma-ray Flashes

In 2005, over ten collaborative research projects began which correlate RHESSI TGF data to radio atmospherics from lightning, optical emission from sprites and elves seen with ISUAL on FORMOSAT-2, relativistic electrons seen with SAMPEX, and even infra-sound from sprites. RHESSI TGF times and locations are now made publicly available in near realtime. RHESSI is the only observatory currently detecting TGFs and releasing TGF data to the community, so it is critical to the progress of this young field over the next several years.

2.2.9 Astrophysical Objectives

The cosmic gamma-ray burst and other transient studies will continue to exploit the unique timing, spectral resolution, and broad energy coverage of RHESSI. In addition, we will continue to image the Crab Nebula and work on improving the aspect solution (the key to obtaining groundbreaking maps) for those solar off-pointings. The inner features of the Crab Nebula are extremely dynamic, showing significant variations from season to season in the optical (HST) and soft X-ray (Chandra) bands (Hester, J. J. et al. 2002). Since the highest energy emission might be expected to be dominated by freshly shock-accelerated particles, this variation could be greatest in RHESSI's hard X-ray band. We therefore plan to revisit the Crab for about one week annually at the Sun's closest approach each June.

Hester, J. J. et al. 2002, ApJ 577, L49

2.2.10 Proposed Solar High-Energy Events GI Program

The new HGO missions – Hinode, STEREO, and SDO later this year – as well as GLAST, provide a near ideal and remarkably complete set of complementary measurements to RHESSI for the study of particle acceleration in solar flares, CMEs and SEPs. These are topics of particular relevance to NASA's Vision for Space Exploration and the Living With a Star initiative. Each of these missions contributes fundamental new insights, but a global integration and analysis of these observations will provide the real pay-off in our understanding of these phenomena. Since the in-guide funding levels of the individual missions are inadequate to cover such integrated studies, we propose a Guest Investigator (GI) program in the coming years to stimulate rapid advancement of our understanding of high-energy solar events - the buildup, initiation, evolution, and consequences of particle acceleration in explosive and eruptive events.

2.3 Potential for Performance during FY-09 to FY-12

2.3.1 Relevance to HP Research Objectives

RHESSI is directly relevant to achieving NASA's strategic goal for Heliophysics to "Understand the Sun and its effects on the Earth and the solar system." It addresses the SMD Science Question - "How and why does the Sun vary?" and the following Research Objectives:

- Understand the fundamental physical processes of the space environment from the Sun to Earth.
- Develop the capability to predict the extreme and dynamic conditions in space in order to maximize the safety and productivity of human and robotic explorers.

2.3.2 Impact of Scientific Results

RHESSI scientific results have been presented at innumerable scientific meetings and published in over 670 papers listed at the following web site:

http://www.lmsal.com/~aschwand/publications/rhessi.html

Many of them are available electronically in the E-Print archive at the Max Millennium web site -

http://solar.physics.montana.edu/max_millennium/

Over 30 PhD and masters degrees that include significant analysis of RHESSI observations have been awarded to date or are in preparation –

http://www.lmsal.com/~aschwand/publications/rhessi_phd.html

2.3.3 Spacecraft and Instrument Health

See Section 3.

2.3.4 Productivity, and Vitality of Science Team

Various awards have been given to members of the RHESSI team in recognition of their contribution to the success of this mission. The PI, Bob Lin, was elected to the National Academy of Science and the American Academy of Arts and Sciences. The PI and CoI, Hugh Hudson, received the AAS/SPD Hale prize in 2005, and 2008, respectively. CoI, Gordon Holman received the 2007 SPD Popular Writing Award for a Scientific American article entitled "The Mysterious Origins of Solar Flares" that included RHESSI results.

The most newsworthy results have been broadcast to the general public through over ten press releases from NASA, UC Berkeley, and UC Santa Cruz covering such topics as magnetic reconnection powering solar flares, the connection between flares and CMEs, the first gamma-ray image of a solar flare, particle acceleration in the large flare on Jan. 20, 2005, the brightest gamma-ray burst ever recorded on Dec. 27, 2004, and terrestrial gamma-ray flashes.

RHESSI personnel have initiated, organized, and attended many scientific meetings and special sessions. In the last three years, the series of international RHESSI workshops continued with events in Paris, France (June 2006), and Santa Cruz, CA (June 2007). Each workshop was attended by some 50-60 scientists. "Topical" RHESSI workshops also took place in Paris, France (April 2006) and Berkeley (2007). RHESSI team members played key roles in several collaborative conferences, such as the one entitled "Solar & Space Physics and the Vision for Space Exploration" held in Wintergreen, VA, in October 2005. Another such joint meeting is being planned on "Anticipating Solar Cycle 24" in Napa, CA, in December 2008. Several international teams of scientists have met in Bern, Switzerland, under the sponsorship of the International Space Science Institute, to explore issues related to RHESSI's hard X-ray spectroscopy and imaging spectroscopy, for example.

Scientists who have attended the RHESSI workshops are preparing a series of papers for a complete ~500-page volume of Space Science Reviews (also to be published as a book) detailing the current state of understanding of all aspects of high-energy solar flares. The chapter titles (with the lead authors in brackets) are as follows:

- An Observational Overview of Flares (Fletcher),
- Interpretation of Thermal and Nonthermal Electron Distributions (Holman),
- Ion Acceleration and Interaction (Vilmer),
- Correlative Radio and Hard X-Ray Observations (White),
- A Statistical Study of Flare Parameters (Hannah),
- Deducing Electron Properties from Hard X-Ray Observations (Kontar),
- Theoretical Implications (Vlahos).

The papers will be ready for joint publication in the summer of 2008.

RHESSI team members have organized special sessions on high-energy solar physics topics at every meeting of the AAS/SPD since launch and at COSPAR General Assemblies. The latest is being organized by CoI, Gordon Holman, at the Montreal COSPAR meeting in July, 2008. In addition, the RHESSI team has held a series of workshops to educate the scientific community on how to use the RHESSI data analysis software in order to obtain the best possible images and spectra.

Members of the RHESSI team helped to organize and served as faculty members for the AAS/SPD Summer School on high-energy solar physics held in Durham, NH, in June 2006. This 10-day summer school was jointly funded by NASA and NSF and was attended by 50 students and postdocs.

2.3.4.1 Science Nuggets

Beginning in March 2005, we began putting a biweekly series of RHESSI "science nuggets" on the following web site:

http://sprg.ssl.berkeley.edu/~tohban/nuggets/

Each nugget is a brief report that is intended to introduce various aspects of the scientific material to a technically competent audience. The Web format allows us to include images, movies, and links. At the time of writing (February, 2008) there are 68 nuggets online with over 50 different authors. The Webmaster is Steven Christe; CoI Hugh Hudson serves as general editor and default writer in case of schedule gaps. The Nuggets are announced in community newsletters that

go to an audience of perhaps 500. Email feedback shows a readership that is both within and outside the solar physics community.

2.3.5 Future Promise

RHESSI is still fully operational and shows tremendous promise for the coming years of increasing solar activity and joint observations with the newer solar missions now in orbit or to be launched in the next year. RHESSI continues to be the only mission capable of solar HXR imaging spectroscopy and is likely to retain that unique position until the launch of the Spectrometer Telescope for Imaging X-rays (STIX) on the Solar Orbiter in 2015. RHESSI's gamma-ray imaging spectroscopy capabilities are not likely to be duplicated or improved on for many years. Thus, it is critical that RHESSI be fully supported for as long as possible to provide the high-energy coverage of the flares that will be seen in increasing numbers with the new and advanced instrumentation on Hinode, STEREO, SDO, and GLAST.

With the successful anneal and the recovery of useable energy resolution and sensitive volume in all of the germanium detectors, RHESSI is ready to make continued observations of X-rays and gamma-rays for at least two more years. Additional anneals will be necessary as the effects of radiation damage build up again. Ground tests with a spare germanium detector indicate that at least four anneals of the same duration and temperature as the one just completed can be safely carried out without endangering the detector segmentation. The cryocooler, while showing signs of degrading performance, is still maintaining the detectors at the acceptable temperature of 90 – 95 K with an input power of 75 watts and negligible microphonics.

2.3.6 Data Accessibility and Usability

Full details of RHESSI data accessibility and usability are given in the accompanying Mission Archive Plan. The data archive contains the full Level-0 telemetry data, the RHESSI flare list, and a number of 'quicklook products' including prepared lightcurves, spectra, and images, and summaries of housekeeping data for the entire mission. The archive, currently ~4.5 TB, resides on three servers, at SSL, Goddard, and at ETH in Zurich, Switzerland. It is online, available, and easily accessible by anyone with an Internet connection. The complete RHESSI software package necessary for the analysis of all RHESSI data is also freely available online as part of the Solar Software (SSW) tree. It is mostly written in the Interactive Data Language (IDL licensed from ITT Visual Data Solutions) and is fully compatible with both UNIX and Windows operating systems.. It contains all procedures necessary to read and unpack the FITS data files, prepare and plot light curves, reconstruct images, and accumulate, display, and analyze spectra. For the expert analyst, the procedures can all be invoked from the IDL command line, but a more user-friendly graphical user interface is also available capable of carrying out all the basic analysis tasks.

There is extensive documentation online at the RHESSI web site –

http://hesperia.gsfc.nasa.gov/rhessi/

that describes the mission, the instrument, the science objectives, data analysis techniques, the software, and the data archive. In addition, there are support personnel at all three sites to guide scientists in using the software and interpreting the results.

2.3.6.1 Browser

To allow for quick inspection of the RHESSI data, there are many automatic routines to produce plots such as quicklook lightcurves and images and detector monitor rates. Navigating this wealth of automatically generated plots is accomplished using a web-based data browser, simply called Browser, found at:

http://sprg.ssl.berkeley.edu/~tohban/browser/

Originally written by graduate student Albert Shih in 2003 and significantly upgraded in 2005, Browser is a powerful tool that allows the user to load a variety of plots relevant for a specified time, and then easily step back and forth through time as desired. Browser also provides the capability of storing the current view as a URL for ease of sharing among researchers. Finally, Browser dynamically generates links to non-RHESSI web-based databases (such as magnetograms) corresponding to the specified time so that the user can investigate the context of the RHESSI data.

2.3.6.2 Facilities for Multi-wavelength Analysis

To achieve the full scientific potential of RHESSI data and to support the convenient integration of RHESSI data into studies initiated in other wavelength regimes, it is essential to have convenient access both to the data from other instruments and to the relevant software resources. Two steps have been taken to ensure this. First, the RHESSI software package includes flexible tools for accessing and integrating multiple data sets (for example by overlaying images). Coalignment is simplified since the absolute positions of RHESSI images are inherently determined to arcsecond accuracy.

Second, we have established a comprehensive RHESSI Synoptic Data Archive at the GSFC Solar Data Analysis Center (SDAC) that allows ready access to a broad range of observations for all the RHESSI flares. The archive contains image, spectrum, and lightcurve data from a wide range of sources stored in

standard formats for direct comparison with RHESSI data. The sources include SOHO (EIT and MDI), TRACE, Big Bear Solar Observatory, Kanzelhohe, and Kiepenheuer Hα full-disk images; GOES-12 SXI full-Sun images and GOES 6-12 two-channel light curves with 3 s time resolution; and Phoenix, Owens Valley Solar Array, Nobeyama, and Nancay radio images and spectra.

We are continuously improving the Synoptic archive as follows:

- Increasing the cadence and time coverage of complementary data to encompass pre- and post-flare phases of GOES and RHESSI-observed events.
- Facilitating access to data from new missions as they become available after launch. We have partnered with the STEREO and Hinode science teams to integrate their data analysis tools into the RHESSI analysis software to permit joint analysis of multi-wavelength observations. We will extend this effort to include next generation data from the Solar Dynamics Observatory (SDO)
- Evolving from a centralized synoptic data archive to a distributed system that is incorporated into the Virtual Solar Observatory (VSO). We have teamed with the SDAC to develop an IDL client interface that directly searches and retrieves VSO datasets. By incorporating this interface into the RHESSI analysis software, we are augmenting the range of different solar observations accessible for joint analysis with RHESSI, while simultaneously extending the data analysis capability of the VSO.

3 TECHNICAL STATUS

3.1 Observatory

RHESSI was launched on February 5, 2002, into a circular orbit with an altitude of 600 km and an inclination of 38°. The observatory continues to function very well after more than 6 years of operations in its present 575 x 554 km orbit. All of its subsystems are fully operational. The solar array power output has declined by only 1.1% since launch, the battery voltage has been stable for the past 2 years, the absolute battery pressure has been stable for the past 3 years, and the differential pressure has been relatively stable for the past 1.5 years. The average spacecraft temperature has increased by only ~1° C since launch. The S-band transceiver still generates a stable output power of 4.9 W with clean BPSK modulation at 4.0 Mbps, and the receiver shows no signs of deterioration in performance. The attitude control system is stable and the command and data handling subsystem shows no signs of degradation.

The CPU experienced six resets since launch. Three of these resets occurred as a result of the very large solar flare in October of 2003, two were caused by watchdog timeouts during ATS loading, and one had an unknown cause. The IDPU never reset autonomously, but was reset once by ground command. On two occasions ATS loads with faulty checksums were erroneously accepted by the spacecraft. However, these ATS loads were subsequently reloaded and verified flawlessly prior to their on-board execution.

Overall, there is no reason to believe that the spacecraft will not continue to function very well over the next three years. The solar arrays have shown minimal degradation and are projected to be capable of providing adequate power for the next three years and beyond. The battery showed some degradation early in the mission, but has been stable for the past two years and is projected to provide adequate power storage for the next several years. The telecommunications subsystem has been stable since launch, and all other subsystems and sensors are functioning nominally.

3.2 Instruments

3.2.1 Spectrometer and Cryocooler

The RHESSI germanium spectrometer and its Sunpower cryocooler continue to work well. Prior to annealing the detectors in Nov. 2007, all nine RHESSI detectors were segmented and functioning. The detectors had suffered radiation damage from trapped and cosmic ray protons at very close to the rate predicted before launch. This only affects the measurements of narrow gamma-ray lines, and has no effect on the performance at soft or hard X-ray energies, to which the vast majority of flares are restricted. At gamma-ray energies, the result was a loss of energy resolution (to approximately 8.1 keV FWHM at 2.2 MeV versus 4.4 keV early in the mission) and a loss of active detector volume (about 15%, with larger changes in some detectors than others).

Three of the detectors, (#2, 5, and 6) have occasionally demonstrated transient noise and current spikes so that their operating voltages have been gradually lowered. (Radiation damage may be responsible for this, but it allows the detectors to remain segmented and operable at lower voltages than would have been possible at launch).

RHESSI's cooler has been powered continuously since the first week of the mission, logging more than 50,000 hours of failure-free operation. It has proven to be relatively easy to adjust the amplitude and phase of the compensating balancer attached to the cooler to reduce the vibration level so that microphonics do not degrade the detector energy resolution.

The cooler has been used twice to cool down the spectrometer detectors and cold plate, from room temperature on the initial cool down, and from 100º C after the anneal cycle in Nov. 2007. It was operated continuously in its standard constant-amplitude mode at ~65 watts from the first week of the mission until the anneal process began. For reasons that are still not completely understood, the average detector temperature has risen from 75K after the initial cool down to approximately 90K just prior to the anneal. (The temperature of the detectors fluctuates ~5 K as the fraction of time in sunlight varies with the orbital precession.) Since the anneal, the cryocooler has been operated at ~75 watts to maintain the coldplate temperature at between 90 and 95 K.

Most of the rise in temperature occurred over the first two years of operation, stabilizing when the spectrometer's insulating vacuum volume was vented to space on Feb. 5, 2004. By implication, there was probably condensable contamination in the spectrometer vacuum volume causing degradation of its thermal performance. Opening the vent probably stopped further accumulation of condensables, but did not release anything already deposited on the spectrometer's interior thermal surfaces.

The cryocooler was kept powered on at ~50 W during the anneal process to keep its own components cool and to prevent damage from excess heat. However, it was operated during that time at an input power that was higher than its design capability at the actual temperatures reached, and it appears that it may have suffered some degradation in performance as a result. For subsequent anneals, the cryocooler will be operated at a lower power setting when the cold-tip temperature is elevated, more closely matching the profile used successfully during initial cool down after launch. The cryocooler performance has stabilized since the anneal, and the coldplate temperature is being maintained at between 90 and 95 K after increasing the input power to 75 watts.

3.2.2 Detector Annealing

The germanium detectors were annealed for the first time in November 2007 to reduce the effects of radiation damage caused by energetic protons and neutrons interacting in the germanium crystals. This involved heating the detectors to a temperature of ~90° C for 7 days. This also vents to space accumulated water ice and other volatiles in the cryostat.

Radiation damage causes two problems: trapping of holes as charges liberated by a gamma-ray drift through the crystal, and creation of charge sites in the crystal that compete with the externally applied electric field. Hole-trapping causes loss of energy resolution due to incomplete charge collection. Charge sites, once present in sufficient number, can actually make part of the detector volume passive by canceling or reversing the applied field. Both of these problems had become severe by 2007.

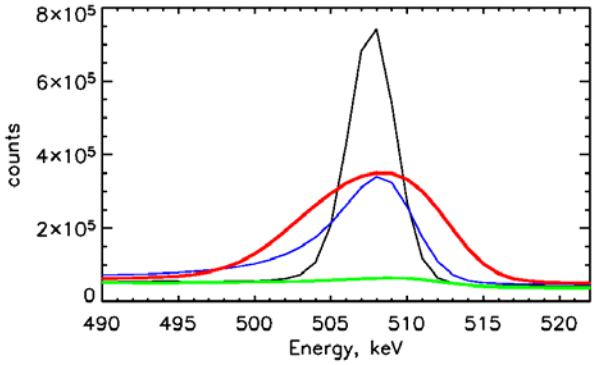

Figure 3.2.2-1. Background gamma-ray line at 511 keV as seen at the start of the mission in early 2002 (black), in mid 2006 (blue), in mid 2007 (shortly before the anneal in green), and at the present time (January 2008 in red).

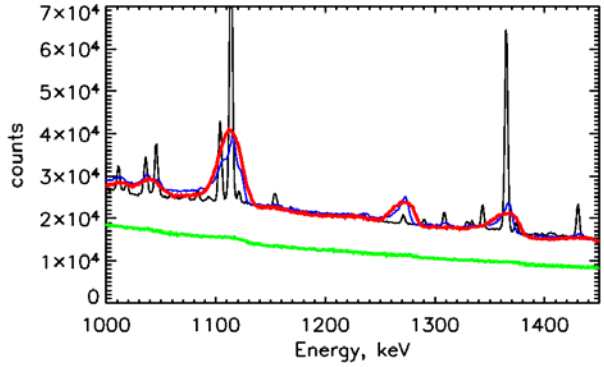

Fig. 3.2.2-2. RHESSI rear segment response to background lines before anneal (green) and after anneal (red). Black shows the performance at the start of the mission in 2002, and blue shows the performance in mid-2006. The full volume and efficiency of the detectors has been recovered, if not the full resolution.

When the detectors were cooled back down to their operating temperature, all but one of the detectors (#2) showed considerable improvement in performance. Approximately half the accumulated radiation damage was effectively removed. All front segments have nearly their full effective area again, and most rear segments are now capable of observing nuclear lines effectively. Neither was the case before the anneal. This will allow high-resolution X-ray and gamma-ray observations of solar flares to be continued. Detector #2, which has been anomalous since launch, is currently operational only as a front segment, with reduced resolution and effective area; this was also the case through much of the pre-anneal mission.

Fig. 3.2.2-1 shows the RHESSI rear segment response to the background 511 keV line just before and after the anneal. Figure 3.2.2-2 shows similar results for lines at higher energies (the sodium background line at 1275 keV builds up slowly over the mission so it is not a good point of comparison for line sensitivity). Although the energy resolution is worse than it was in 2002, the *efficiency* for collecting lines is completely recovered. Since most solar lines are naturally broadened, the most important part of the recovery has been achieved. Even the current resolution is many times better than previous missions, such as SMM/GRS, that used scintillators instead of germanium.

By mid-2007, many front segments had lost effective area due to radiation damage, particularly detector 5. Analysis of the X-ray count-rate spectra for three C-class flares detected in 2005, 2007 -pre-anneal, and 2007 post-anneal shows that most of this loss has been recovered by the anneal in all detectors but #2 and 7 that have always had degraded energy resolution and a higher threshold since launch.

We expect to execute at least one more anneal cycle, probably to be performed around late 2009, as solar maximum approaches and the detectors reach a similar level of damage as just before the recent anneal. The amount of annealing we can do is limited by the drift of implanted lithium ions at the inner bore of the detectors. The segmentation of the RHESSI GeDs is caused by a gap in the inner electrical contact, which is made conductive by the lithium. At high temperatures, the lithium becomes mobile in the Ge crystal and can drift so as to close the gap. This would desegment the detector and cause several problems for its performance, but it could still be operated as an unsegmented detector. We have repeatedly annealed a spare detector in the laboratory, and it began to desegment after approximately one month at 95° C. We are therefore confident that a second anneal of 1 to 2 weeks will be possible without desegmenting the flight detectors.

3.2.3 Imager

The RHESSI imager subsystem consists of nine rotating modulation collimators, each of which has a pair of widely separated grids. A metering structure maintains the relative twist alignment of the nine grid pairs. The imaging subsystem is inherently stable and has shown no evidence of change in grid alignment. Improved analysis techniques are refining the calibration of the grid parameters and locations (now known to submicron accuracy), the results of which are built into the software package and are applicable to all data acquired since launch.

3.2.4 Aspect System

There are three parts to the RHESSI aspect system. The absolute pitch and yaw angles relative to Sun center are provided by the Solar Aspect System (SAS), with sub-arcsecond accuracy. The spacecraft roll angle is provided by two redundant side-looking star scanners, a CCD-based Roll Angle System (RAS) and a Photomultiplier-Tube-based Roll Angle System (PMTRAS).

The SAS consists of a set of 3 identical lens/sensor subsystems each of which focuses a narrow-bandwidth image of the solar disk onto a linear CCD array. No anomalies in its operation have been observed. During the first few months of the mission, the sensitivity of the SAS decreased, but it has now stabilized at ~60% of the original value, a level which provides an order of magnitude of sensitivity margin with no compromise in accuracy. The SAS also continues to provide accurate radius measurements (to 50 mas) for the study of global solar applications as discussed in section 2.1.7.

The PMT-RAS continues to provide the roll aspect knowledge upon which most of the solar imaging is based. Its response has remained stable since launch, easily meeting its 1 arcminute roll-angle requirement with a large margin in sensitivity.

The CCD-based RAS has also proven to be stable and able to meet the 1 arcminute roll-angle requirement. CCD-RAS data are used to fill occasional gaps in the PMT-RAS coverage. In addition, by measuring the polar angle as well as the roll angle, the CCD-RAS can provide full aspect information with 10 arcsecond accuracy for non-solar targets such as the Crab nebula and the pulsar A0535+26.

3.3 Software

One of the unique characteristics of RHESSI is that the telemetered data contain detailed information on each detected photon. This provides unprecedented flexibility in that decisions and tradeoffs associated with time resolution, energy resolution, imaging resolution and field of view, etc, can be made *ex post facto*, enabling the analyst to make these decisions in the manner best suited to the scientific objectives and to the characteristics of the event under study. The RHESSI software fully supports this flexibility. Another advantage of this photon-oriented database is that ongoing improvements to the software and instrument calibration can be fully applied retroactively to all the data since the beginning of the mission.

The RHESSI software package is well-developed, robust, and available via SolarSoft. It can be used with the IDL command line, a user-friendly graphical user interface, or scripts for automating user-specific tasks. The software generates images, and spatially-integrated

or feature-specific spectra and light curves and provides full support for comparisons with data products from other missions. Recent developments have included the fully-integrated generation and analysis of image cubes as a function of time and/or energy to better support imaging spectroscopy. Many important improvements have been made to the spectral analysis capabilities, and software has been developed to calculate visibilities and to carry out visibility-based analyses. The gamma-ray detector response is also being modified to better account for Compton scattered photons in the detectors.

Visibilities are calibrated, 'instrument-independent,' Fourier components of the source image. Mathematically, they correspond to the output of a single baseline of a radio interferometer. For RHESSI, they represent an intermediate data product directly obtained from the observed time-modulated light curves. Visibility measurements have well-defined statistical errors. Their value lies in the fact that they depend linearly both on the data and on the source. Consequently, they can be flexibly combined for comparison between source models and observations. The basic visibility software implemented to date has enabled the accurate determination of hard X-ray source sizes (useful for example to convert thermal emission measurements to electron densities), and the evaluation of albedo; it was the computational tool of choice in obtaining several of the recent results discussed in section 2. Refinements in the calculation of visibilities and in their use for other applications (such as improved spectral line imaging, albedo analysis, and subsecond time resolution studies) are priority goals of the ongoing software development effort.

3.4 Ground System

In 1999, a multi-mission operations facility was established at SSL to support the RHESSI and FAST missions. The joint facility, which now also supports CHIPS and THEMIS operations, includes the Mission Operations Center (MOC), the Science Operations Center (SOC), the Flight Dynamics Center (FDC), and the Berkeley Ground Station (BGS). A high degree of integration and automation combined with flexible system architecture provides a reliable and cost effective state-of-the-art environment to perform all functions required to operate multiple spacecraft simultaneously.

3.4.1 Ground Stations

The primary ground station for the RHESSI mission is BGS. Backup support is provided by the Wallops Island (WGS), Santiago (AGO), Merritt Island (MILA), and the DLR ground station at Weilheim, Germany. BGS has supported more than 12,000 RHESSI passes since launch - on average 5-6 passes per day. WGS, AGO and MILA support typically 4 passes per day combined. The average daily data volume is 13.5 Gbits with an overall telemetry recovery efficiency of ~99%.

The BGS consists of an 11-m parabolic reflector mounted on a pedestal with a three-axis drive system, and an S-band RF system. Since the azimuth and elevation gear boxes were rebuilt after a failure in 2002, BGS operations have been very reliable, supporting more than 21,000 passes for RHESSI, FAST, CHIPS and THEMIS combined.

3.4.2 Mission Operations Center

The RHESSI Mission Operations Center is part of a secure, shared state-of-the-art facility with a network of workstations for flight dynamics, spacecraft command and control, mission planning, command load generation, and data trending. The facility, typically staffed during normal working hours only, performs automated pass supports, spacecraft and instrument state-of-health checks, and generation of all ephemeris and planning products in a lights-out mode.

3.4.2.1 Normal Operations

RHESSI normal operations comprise mission planning functions, command load generation, real-time pass supports, spacecraft state-of-health monitoring, data trending, instrument configuration, and science data recovery and archiving. Generation of all ephemeris and mission planning products is based on two-line element sets that are downloaded from the Space-Track.org web site, quality checked and archived locally in a fully automated mode. Spacecraft ATS loads are built by the FOT and uploaded to the spacecraft multiple times per week. Every six weeks, the spacecraft is re-spun from about 14.5 rpm to its nominal spin rate of 15 rpm. The FOT works closely with project scientists to determine the optimal instrument configuration consistent with the current level of solar activity.

During off-hours, FOT members carry two-way pagers to receive notifications regarding any spacecraft or ground system anomalies. A number of web-based tools allow FOT members, subsystem engineers, and instrument scientists to monitor spacecraft and instrument performance remotely.

Since RHESSI is operated from a multi-mission facility, its resources are shared with other missions. This approach provides redundancy and reduces overall operations costs. The flight control team now operates RHESSI, FAST, CHIPS, and THEMIS for a total of 8 spacecraft.

3.4.3 Science Operations Center

The RHESSI SOC, located at SSL, consists of three RAID servers, with ~6.1 Tbytes of data capacity, and six processors. The SOC receives RHESSI data after every ground-station contact and automatically processes them to create the Level-0 data files. As of late February 2008 there are approximately 54,500 Level-0 data files, containing 4 Tbytes of data, for an average of approximately 1.8 Gbyte of data per day.

Other automated procedures generate quick-look data containing the RHESSI observing summary, flare list, and quick-look light curves, images, and spectra. Long-term trend plots of SOH data are updated daily in the SOC. All of these data products are available through the RHESSI Data Center website at Goddard -

http://hesperia.gsfc.nasa.gov/rhessidatacenter/

3.4.4 Max Millennium Program

The RHESSI PI team created and supports the Max Millennium program for several functions that are key to the successful acquisition of observationally complete datasets and the full scientific exploitation of those observations. These functions are accessible at

http://solar.physics.montana.edu/max_millennium/

They include the following:

1. Joint observing plans between RHESSI and other instrumentation with specific scientific goals.
2. Daily observing targets generated each day by one of four experienced solar observers (the Max Millennium Chief Observers)
3. RHESSI data analysis projects submitted by active scientists interested in collaborations.
4. RHESSI software and hardware updates.
5. The Solar Physics E-Print Archive. A recent study indicates that papers in this archive are cited about twice as often as average.
6. Majordomo email for items of interest going to 353 self-subscribed participants.

3.4.5 Education and Public Outreach

RHESSI E/PO will continue its partnership with the programs of the Center for Science Education and the Space Sciences Laboratory (CSE@SSL) to provide professional development opportunities and classroom support for teachers in Northern California and at National Conferences. We will also collaborate with CSE@SSL programs that reach out to informal education venues and community groups, such as museums during the annual Sun-Earth Day events and *Traditions of the Sun* community events. RHESSI has produced an informal *Exploring Magnetism in Space Science* kit for these kinds of venues.

We will partner with THEMIS and AIM E/PO to train and support a cohort of Heliophysics Educator Ambassadors. These teachers will be selected from teachers in the AIM E/PO and THEMIS GEONS programs and will receive information about Heliophysics missions, training on quality classroom materials developed by NASA and best practices in teacher professional development. The teachers will act as Heliophysics Ambassadors with teachers in their local regions across the country. In addition, RHESSI E/PO will partner with other missions in the Heliophysics division to collect all the best classroom resources they have developed and organize them into a "curriculum" that can be used for the Heliophysics Educator Ambassador program. RHESSI will continue to disseminate its electronic E/PO resources via its website and CD-ROMs produced in partnership with THEMIS, FAST, and STEREO-IMPACT E/PO.

At Goddard, we will continue to combine resources with other HD missions with a presence here including SOHO, Cluster, Wind, STEREO, and Hinode, and the upcoming SDO mission. These efforts will be coordinated by the new hire in the Heliophysics Science Division whose duties will include leading and coordinating the Education and Public Outreach activities of the division.

4 APPENDICES

4.1 Budget

4.2 Acronym List

AAS	American Astronomical Society
ACS	Attitude Control System
AESP	Aerospace Education Services Program
AGO	Santiago ground station
AGU	American Geophysical Union
AIM	Aeronomy of Ice in the Mesosphere
AISES	American Indian Science and Engineer Society
ATS	Absolute Time Sequence
AU	Astronomical Unit
BATSE	Burst and Transient Source Experiment on CGRO
BGO	Bismuth Germinate used as a scintillation detector
BGS	Berkeley Ground Station
BPSK	Binary Phase Shift Keying
CAST	CERN Axion Solar Telescope
CCD	Charge Coupled Device
CD-ROM	Compact Disk – Read Only Memory
CHIPS	Cosmic Hot Interstellar Plasma Spectrometer
CGRO	Compton Gamma Ray Observatory
CME	Coronal Mass Ejection
COMPTEL	Compton Telescope on CGRO
COR-1	Inner Coronograph of STEREO SECCHI instrument
COR-2	Outer Coronograph of STEREO SECCHI instrument
COSPAR	COmmittee on SPAce Research
CSE@SSL	Center for Science Education at Space Sciences Laboratory
CSTA	California Science Teachers Association
DLR	Weilheim ground station
EGRET	Energetic Gamma Ray Experiment Telescope on CGRO
ERC	Educator Resource Center
EEPROM	Electrically Erasable Programmable Read-Only Memory
EIT	Extreme Ultraviolet Imaging Telescope on SOHO
EIS	EUV imaging spectrograph on Hinode
E/PO	Education and Public Outreach
ETH	Eidgenossische Technische Hochschule, Zurich, Switzerland
EUV	Extreme Ultra-Violet
EVA	Extra-Vehicular Activity
FAST	Fast Auroral SnapshoT
FDC	Flight Dynamics Center
FIP	First Ionization Potential
FITS	Flexible Image Transport System
FORMOSAT-2	Earth Observation Satellite
FOT	Flight Operations Team
FoV	Field of View
FTE	Full time Equivalent
FWHM	Full Width at Half Maximum
GDS	Ground Data System
Ge	Germanium
GeD	Germanium Detector

GEMS	Great Explorations in Math and Science
GEONS	Geomagnetic Event Observation Network by Students
GLAST	Gamma-ray Large Area Space Telescope
GRB	Gamma Ray Burst
GRS	Gamma Ray Spectrometer
GSFC	Goddard Space Flight Center
G/T	Antenna gain to noise temperature ratio
HD	Heliophysics Division
HEAD	High Energy Astrophysics Division
HGO	Heliophysics Great Observatory
Hinode	Japanese solar satellite - formerly Solar-B
HST	Hubble Space Telescope
HXR	Hard X-ray
HXT	Hard X-ray Telescope on Yohkoh
IDL	Interactive Data Language
IDPU	Instrument Data Processing Unit
IGES	Institute for Global Environmental Strategies
IMPACT	In-situ Measurements of Particles and CME Transients on STEREO
IPM	Interplanetary Medium
ISUAL	Imager of Sprites and Upper Atmospheric Lightnings on FORMOSAT-2
ITOS	Integrated Test and Operations System
KSC	Kennedy Space Center
LASCO	The Large Angle and Spectrometric Coronagraph on SOHO
LAT	Large Area Telescope on GLAST
LHCP	Left-Handed Circular Polarization
LHS	Lawrence Hall of Science
LSEP	Large SEP event
mas	milli-arcsecond
MDI	Michelson Doppler Imager on SOHO
MILA	Merritt Island ground station
MOC	Mission Operations Center
MOU	Memorandum of Understanding
MPS	Mission Planning System
NaI	Sodium Iodide used as a scintillation particle detector
NASA	National Aeronautics and Space Administration
NSTA	National Science Teacher Association
NuSTAR	Nuclear Spectroscopic Telescope Array
OCA	Orbital Carrier Aircraft
OIG	Orbital Information Group
PD	Professional Development
PMTRAS	Photomultiplier Roll Angle System
PSLA	Project Service Level Agreement
RAD6000	Radiation-hardened single board computer used on spacecraft
RAS	Roll Angle System
RF	Radio Frequency
RHCP	Right-Handed Circular Polarization
RHESSI	Reuven **R**amaty **H**igh **E**nergy **S**olar **S**pectroscopic **I**mager
SAA	South Atlantic Anomaly
SACNAS	Society for Advancement of Chicanos and Native Americans in Science
SAMPEX	Solar Anomalous and Magnetospheric Particle Explorer
SAS	Solar Aspect System
SatTrack	Satellite Tracking software
SDAC	Solar Data Analysis Center
SDO	Solar Dynamics Observatory
SECCHI	Sun Earth Connection Coronal and Heliospheric Investigation on STEREO
SECEF	Sun Earth Connection Education Forum

SEGway	Science Education Gateway
SEP	Solar Energetic Particles
SEPT	Solar Electron Proton Telescope on STEREO / IMPACT
SERS	Spacecraft Emergency Response System
SHH	Soft, Hard, Harder – spectral evolution
SHS	Soft, Hard, Soft – spectral evolution
SMEX	NASA's Small Explorer Program
SMM	Solar Maximum Mission
SOC	Science Operations Center
SOH	State-Of-Health
SOHO	Solar and Heliophysics Observatory
SOT	Solar Optical Telescope on Hinode
SPD	Solar Physics Division
SSL	Space Sciences Laboratory
STE	Suprathermal Electron Telescope on STEREO / IMPACT
STEREO	Solar TErestrial RElations Observatory
STIX	Spectrometer Telescope for Imaging X-rays
SSW	SolarSoftware
STEM	Science, Technology, Engineering, and Math
SXI	Soft X-ray Imager
TGF	Terrestrial Gamma-ray Flash
THEMIS	Time History of Events and Macroscale Interactions during Substorms
TRACE	Transition Region and Coronal Explorer
UCB	University of California at Berkeley
UT	Universal Time
VSO	Virtual Solar Observatory
VxWorks	A real-time operating system
WGS	Wallops Ground Station
WISE	Wide Field Infrared Survey Explorer
XRT	X-Ray Telescope on Hinode
Yohkoh	Japanese Solar Observatory Satellite